Inorganic Chemistry

Article

pubs.acs.org/IC

A Stable Planar-Chiral *N*-Heterocyclic Carbene with a 1,1′-Ferrocenediyl Backbone

Alex R. Petrov,[†] Anatoli Derheim,[†] Jan Oetzel,[†] Michael Leibold,[†] Clemens Bruhn,[†] Stefan Scheerer,[‡] Steffen Oßwald,[‡] Rainer F. Winter,[‡] and Ulrich Siemeling*[,†]

[†]Institute of Chemistry, University of Kassel, Heinrich-Plett-Straße 40, 34132 Kassel, Germany

[‡]Fachbereich Chemie, Universität Konstanz, Universitätsstraße 10, 78457 Konstanz, Germany

S *Supporting Information*

ABSTRACT: This paper focuses on the stable, ferrocene-based *N*-heterocyclic carbene (NHC) *rac*-[Fe{(η^5-*t*-BuC$_5$H$_3$)NpN}$_2$C:] (**A′-Np**, Np = neopentyl), which is planar-chiral due to the two *tert*-butyl substituents in 3,3′-positions. **A′-Np** was synthesized in nine steps starting from 1,1′-di-*tert*-butylferrocene (**1**), the first step being its 3,3′-dilithiation to afford *rac*-[Fe(η^5-*t*-BuC$_5$H$_3$Li)$_2$] (*rac*-fc′Li$_2$, **2**). The structures of *rac*-fc′(SiMe$_3$)$_2$ (**3**), *rac*-fc′Br$_2$ (**4**), *rac*-fc′(N$_3$)$_2$ (**5**), and the immediate carbene precursor [**A′-Np**H]BF$_4$ were determined by single-crystal X-ray diffraction (XRD). The chemical properties of **A′-Np** were found to be very similar to those of its *tert*-butyl-free congener **A-Np**, both being ambiphilic NHCs with rather high calculated HOMO energies (ca. −4.0 eV) and low singlet−triplet gaps (ca. 35 kcal/mol). A Tolman electronic parameter value of 2050 cm^{-1} was derived from IR data of *cis*-[RhCl(**A′-Np**)(CO)$_2$], indicating the high donicity of **A′-Np** as a ligand. Consistent with its ambiphilic nature, **A′-Np** was found to react readily with carbon monoxide, affording the betainic enolate (**A′-Np**)$_2$CO as four stereoisomers, viz. (R_pR_p-**A′-Np**)═C(O$^-$)(R_pR_p-**A′-Np**$^+$), (S_pS_p-**A′-Np**)═C(O$^-$)(S_pS_p-**A′-Np**$^+$), (R_pR_p-**A′-Np**)═C(O$^-$)(S_pS_p-**A′-Np**$^+$), and (S_pS_p-**A′-Np**)═C(O$^-$)(R_pR_p-**A′-Np**$^+$). The former two isomers were structurally characterized as a racemic compound by single-crystal XRD. **A′-Np** was found to react swiftly with dichloromethane, affording the addition product **A′-Np**H−CHCl$_2$ in a reaction that is unprecedented for diaminocarbenes. **A-Np**H−CHCl$_2$ was obtained analogously. Both compounds were structurally characterized by single-crystal XRD. An electrochemical investigation of **A′-Np** by cyclic and square wave voltammetry revealed a reversible oxidation of the carbene at a half-wave potential of −0.310 vs ferrocene/ferrocenium (THF/NBu$_4$PF$_6$). The electrochemical data previously published for **A-Np** were identified to be incorrect, since unnoticed hydrolysis of the NHC had taken place, affording **A-Np**(H$_2$O). The hydrolysis products of **A-Np** and **A′-Np** were found to be reversibly oxidized at half-wave potentials of −0.418 and −0.437 V, respectively.

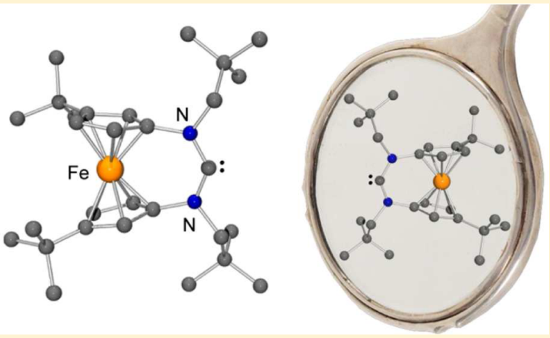

INTRODUCTION

The most widely used *N*-heterocyclic carbenes (NHCs) are based on five-membered heterocycles such as, for example, imidazole and 1,2,4-triazole.[1] NHCs based on heterocycles with larger ring sizes (so-called expanded-ring NHCs) are attracting increased attention.[2,3] Examples with six-, seven-, and even eight-membered rings have been reported. These larger ring sizes lead to comparatively large N−C−N angles, close to that of acyclic diaminocarbenes.[4] This has interesting steric and electronic consequences. The *N*-substituents are pushed in the direction of the divalent C atom, which results in enhanced steric protection of coordinated metal centers. An increase of the N−C−N angle also causes an increase in HOMO energy, and, hence, basicity, nucleophilicity, and σ-donor ability,[5] as is reflected, for example, by comparatively low Tolman electronic parameter (TEP) values of ring-expanded NHCs.[6]

Ferrocene-based, and hence redox-active, NHCs of type **A**, which formally contain a six-membered heterocyclic ring (Figure 1), form a fascinating subclass of expanded-ring NHCs.[7] Utilizing bulky *N*-substituents, viz. 2-adamantyl (Ad) or neopentyl (Np), we succeeded in the synthesis of the first stable examples of such carbenes.[8] Independently from us, analogues with less bulky *N*-substituents (Me, *i*-Bu, Ph) that consequently were too unstable for isolation were published by Bielawski.[9] Their TEP values (2049 ± 1 cm^{-1}) are between

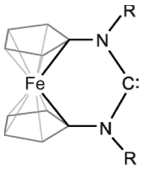

A

Figure 1. Ferrocene-based NHCs of type **A** (highlighting the six-membered heterocyclic ring).

Received: May 12, 2015
Published: June 22, 2015

DOI: 10.1021/acs.inorgchem.5b01064
Inorg. Chem. 2015, 54, 6657−6670

those of six-membered ring NHCs with an all-carbon backbone (2045 ± 3 cm^{-1}) and standard five-membered ring NHCs (≥2050 cm^{-1}).[6,7]

Diaminocarbenes of type **A** are peculiar in several ways. First, they are ambiphilic, which makes them suitable for small-molecule activation.[10] For example, the *N*-neopentyl derivative **A-Np** reacts with CO to afford the betainic enolate (**A-Np**)=C(O^-)(**A-Np**$^+$) (Figure 2) by nucleophilic addition of unreacted carbene to the diaminoketene which is formed as the primary carbonylation product.

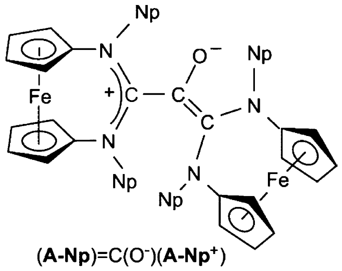

Figure 2. Structural formula of (**A-Np**)=C(O^-)(**A-Np**$^+$), the carbonylation product of **A-Np**.

The only other cyclic diaminocarbene which undergoes a carbonylation reaction with CO is the "anti-Bredt NHC" recently described by Bertrand, which features enhanced electrophilicity that is due to the bridgehead position of one of the two N atoms, which suppresses the π-donation of this amino group.[11] Second, carbenes of type **A** are redox-active. When coordinated to a metal center, their net electron donor capacity can be redox-switched due to a reversible ferrocene-based oxidation. This causes a substantial increase of the TEP value of ca. 11 cm^{-1}, which means that the donor properties become more phosphane-like upon oxidation.[8b,9,12] This behavior can be utilized for redox-switchable catalysis, as was recently demonstrated by Bielawski in olefin metathesis with a ruthenium alkylidene complex containing the methyl-substituted NHC ligand **A-Me**.[9a] In a previous study addressing the redox behavior of the stable 2-adamantyl- and neopentyl-substituted NHCs **A-Ad** and **A-Np**, we have reported that both compounds undergo a quasi-reversible one-electron oxidation with a half-wave potential of ca. −0.42 V vs the ferrocene/ferrocenium couple.[8b] This well-behaved redox process appears remarkable in view of the fact that standard imidazol-2-ylidenes exhibit an irreversible oxidation process at $E_p \approx -0.4$ V vs the same ferrocene/ferrocenium scale.[13] To leak a main result of the present study already at the beginning, the electrochemical data reported in our study of **A-Ad** and **A-Np** were incorrect and are due to a follow-up product, which was rapidly formed inside the electrochemical cell. Interestingly, DFT calculations indicate that the oxidized NHCs **A-Ad**$^{\bullet +}$ and **A-Np**$^{\bullet +}$ are delocalized radical cations, their spin density being approximately equally distributed between the Fe and the carbene C atom.[8b]

We surmised that electron-donating substituents at the cyclopentadienyl rings, which increase the electron density in the ferrocenylene (fc) backbone, would lead to a more localized situation, viz. a ferrocenium-type radical cation, together with a less-perturbed diaminocarbene moiety. This combination

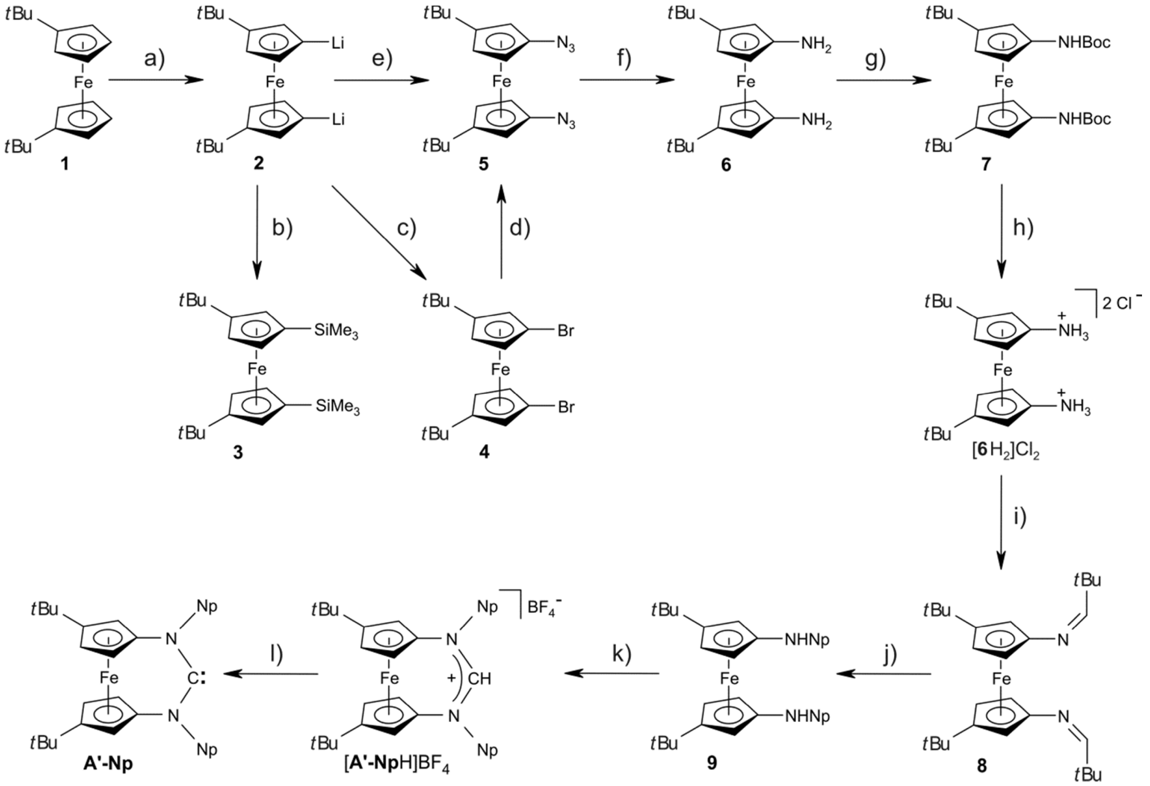

Figure 3. Synthesis of the target NHC **A′-Np** starting from 1,1′-di-*tert*-butylferrocene (**1**). All planar-chiral compounds were obtained as racemates. Only one enantiomer is shown. Reagents and isolated yields (a) *n*-BuLi, TMEDA, 70%; (b) TMSCl, 98%; (c) $(CHBr_2)_2$, 62%; (d) NaN_3, CuI, 81%; (e) TsN_3, 96%; (f) H_2, Pd/C, 95%; (g) Boc_2O, 92% (including step f) without isolation of **6**; (h) AcCl, MeOH, 83% (including steps f and g) without isolation of **6** and **7**; (i) *t*-BuCHO, NEt_3, 92%; (j) $LiAlH_4$, 93%; (k) $HC(OEt)_3$, NH_4BF_4, 52%; and (l) LDA, 83%.

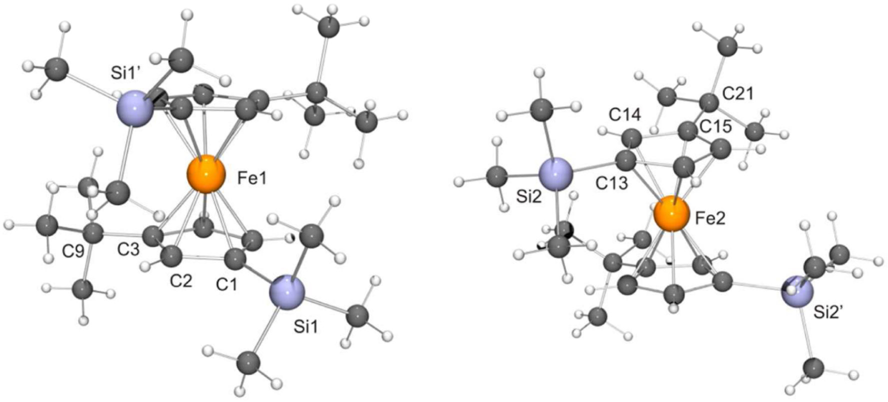

Figure 4. Molecular structure of the S_pS_p enantiomer (left) and the R_pR_p enantiomer (right) of **3** in the crystal. Selected bond lengths: C1−Si1, 1.878(3) Å; C3−C9, 1.521(4) Å; C13−Si2, 1.874(3) Å; and C15−C21, 1.525(4) Å.

promises to give rise to an isolable ferrocenium-based carbene, which would offer the possibility to investigate the influence of the cationic backbone on the carbene reactivity. We chose 1,1′-di-*tert*-butylferrocene (**1**) as the starting point, since the two *tert*-butyl groups have been reported to lead to a substantial cathodic shift of the half-wave potential of −0.30 V in comparison to pristine ferrocene.[14] Our target NHC thus contains the [Fe(C$_5$H$_3$*t*-Bu)$_2$] (fc′), instead of the [Fe(C$_5$H$_4$)$_2$] (fc) backbone, and is therefore denoted as **A′-Np**. Note that the fc′ backbone causes planar chirality in this system.[15]

■ RESULTS AND DISCUSSION

The synthesis of the target NHC is outlined in Figure 3. It was crucial to have easy access to substantial quantities of 1,1′-di-*tert*-butylferrocene (**1**).[14,16] Consequently, we have developed an efficient procedure for its preparation on a large scale from inexpensive starting materials (see the Experimental Section). For the synthesis of the precursor *tert*-butylcyclopentadiene, *t*-BuBr was reacted with potassium cyclopentadienide, which was conveniently generated *in situ* from cyclopentadiene and KO*t*-Bu.[17]

The dilithiation of 1,1′-di-*tert*-butylferrocene (**1**) with *n*-BuLi in the presence of TMEDA is known to occur exclusively in the 3,3′-positions, selectively affording *rac*-1,1′-di-*tert*-butyl-3,3′-dilithioferrocene (*rac*-fc′Li$_2$, **2**) as TMEDA complex. Two different compositions have been reported for this complex, viz. [**2**(TMEDA)$_2$][14] and [**2**(TMEDA)].[18] In our hands, the composition of the isolated product turned out to be [(**2**)$_3$(TMEDA)$_2$], determined gravimetrically through reaction with an excess of Me$_3$SiCl, affording the silylated derivative *rac*-fc′(SiMe$_3$)$_2$ (**3**) in essentially quantitative yield. The same 3:2 ratio has been found by single-crystal X-ray diffraction (XRD) studies for the adduct of 1,1′-dilithioferrocene (fcLi$_2$) with TMEDA.[19] We have tested two different methods for the transformation of dilithiated 1,1′-di-*tert*-butylferrocene to the diazide *rac*-fc′(N$_3$)$_2$ (**5**), which we performed in analogy to the syntheses of fc(N$_3$)$_2$ reported by the groups of Arnold[20] and of Tárraga and Molina.[21] The first option is a two-step procedure. In the first step, the dilithio compound **2** is reacted with 1,1,2,2-tetrabromoethane to give the dibromo derivative *rac*-fc′Br$_2$ (**4**), which is subsequently reacted with sodium azide in the presence of Cu^{I} halide. This method gave **5** in 50% overall yield. The second method proved to be much superior, affording **5** in almost quantitative yield in a single step, viz. by reacting [(**2**)$_3$(TMEDA)$_2$] with tosyl azide. **5** was converted to the corresponding diaminoferrocene *rac*-fc′(NH$_2$)$_2$ (**6**) by catalytic hydrogenation under heterogeneous conditions (H$_2$, Pd/C).[20] **6** is very soluble in common organic solvents. Furthermore, it is a very electron-rich ferrocene derivative and therefore extremely air-sensitive, particularly in solution. This makes purification by standard methods such as column chromatography and crystallization rather cumbersome. Therefore, we chose to convert the diamine **6** *in situ* to the air-stable Boc-protected derivative *rac*-fc′(NHBoc)$_2$ (**7**) by reaction with di-*tert*-butyl dicarbonate (Boc$_2$O). Purification of the protected product was easily possible by column chromatography. Removal of the Boc groups was achieved with HCl generated *in situ* by alcoholysis of acetyl chloride with methanol, according to Nudelman et al.[22] This procedure afforded the hydrochloride [**6**H$_2$]Cl$_2$ in excellent purity. Because of the electron-withdrawing nature of the NH$_3^+$ groups, this hydrochloride is not prone to aerobic oxidation and represents a convenient source of the diaminoferrocene **6**, which can be obtained by treatment of the hydrochloride with a suitable base. The final steps of the synthesis of the target NHC shown in Figure 3 were performed in analogy to the synthesis of **A-Np**.[8b] The condensation of **6** (liberated from its hydrochloride by treatment with triethylamine) with pivalaldehyde afforded the corresponding diimine derivative *rac*-fc′(NH=CH*t*-Bu)$_2$ (**8**), which was converted to *rac*-fc′(NHNp)$_2$ (**9**) by reduction with lithium aluminum hydride. The reaction of **9** with triethyl orthoformate and ammonium tetrafluoroborate furnished the formamidinium salt [**A′-Np**H]BF$_4$. Treatment of this formamidinium salt with LDA in diethyl ether at room temperature afforded the target NHC as a viscous oil, which is very soluble in common organic solvents and could not be crystallized, despite many attempts.

The new compounds (**3**−**9**), as well as the target NHC and its precursor [**A′-Np**H]BF$_4$, were characterized by NMR spectroscopy and high-resolution (HR) electrospray ionization (ESI) mass spectrometry. Satisfactory microanalytical data could be obtained in all cases except the highly air-sensitive and noncrystalline free carbene. In addition, we have determined the crystal structures of *rac*-fc′(SiMe$_3$)$_2$ (**3**), *rac*-fc′Br$_2$ (**4**), *rac*-fc′(N$_3$)$_2$ (**5**), and [**A′-Np**H]BF$_4$ by single-crystal XRD. The molecular structures are shown in Figures 4−7.

The structure of **3** resembles the structures of 1,1′,3,3′-tetra-*tert*-butylferrocene[23] and of 1,1′,3,3′-tetrakis(trimethylsilyl)-ferrocene.[24] The "interlocked" arrangement of the bulky substituents observed in each case may be ascribed to steric

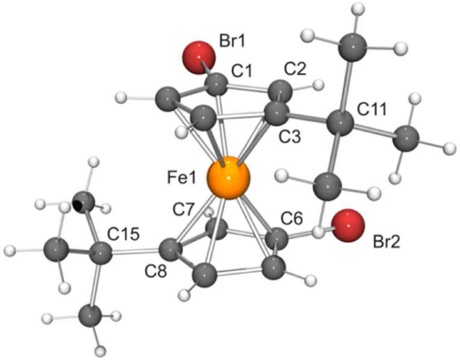

Figure 5. Molecular structure of **4** in the crystal. Selected bond lengths: C1−Br1, 1.896(2) Å; C3−C11, 1.521(3) Å; C6−Br2, 1.890(3) Å; and C8−C15, 1.511(4) Å.

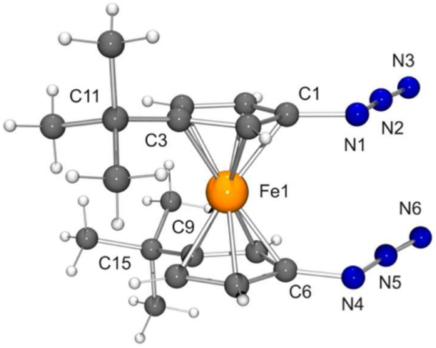

Figure 6. Molecular structure of **5** in the crystal. Selected bond lengths and bond angles: C1−N1, 1.429(6) Å; C3−C11, 1.520(7) Å; C6−N4, 1.428(7) Å; C9−C15, 1.510(8) Å; N1−N2, 1.215(8) Å; N2−N3, 1.137(9) Å; N4−N5, 1.229(8) Å; and N5−N6, 1.150(8) Å; C1−N1−N2, 117.1(4)°; N1−N2−N3, 171.7(6)°; C6−N4−N5, 116.0(5)°; and N4−N5−N6, 172.2(6)°.

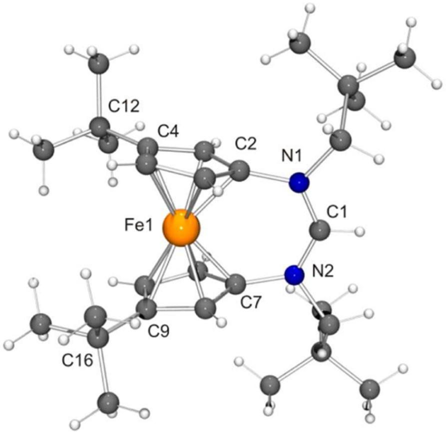

Figure 7. Molecular structure of the cation of [**A′**-**Np**H]BF_4 in the crystal. Selected bond lengths and bond angles: C1−N1, 1.321(4) Å; C1−N2, 1.311(4) Å; C2−N1, 1.430(5) Å; C4−C12, 1.506(6) Å; C7−N2, 1.438(4) Å; and C9−C16, 1.514(4) Å; N1−C1−N2, 131.0(3)°; C1−N1−C2, 123.6(3)°; and C1−N2−C7, 124.7(3)°.

repulsions. Two enantiomeric molecules are present in the asymmetric unit, whose conformations differ significantly. Both have molecular C_2 symmetry. Molecule 1 (S_pS_p enantiomer) has an almost-eclipsed arrangement of the cyclopentadienyl rings (twist angle = 6.3°), which are slightly tilted by 4.7°. When viewed along the axis containing the cyclopentadienyl ring centroids, the order of the substituents of the upper (u) and the lower (l) cyclopentadienyl rings is Me_3C(u)−Me_3Si(l)−Me_3Si(u)−Me_3C(l) (abbreviated as CSiSiC). Molecule 2 (R_pR_p enantiomer) exhibits substantially larger twist and tilt angles of 15.4° and 8.5°, respectively. The order of substituents in this case is Me_3Si(u)−Me_3C(l)−Me_3C(u)−Me_3Si(l) (abbreviated as SiCCSi). The wedge caused by the ring tilt opens up toward the inner two substituents, viz. C*SiSi*C in the case of molecule 1 and Si*CC*Si in the case of molecule 2. The larger ring twist and tilt angles observed for molecule 2 indicate that the steric repulsion between the *tert*-butyl groups (*CC*) in molecule 2 is larger than that between the corresponding trimethylsilyl groups (*SiSi*) in molecule 1, which is further supported by the observation that the *CC* groups in molecule 2 are bent away from the metal center by 8.5°, while the *SiSi* groups in molecule 1 are bent away by only 6.1°. These observations are not at all surprising. It is well-known that the steric effect of a *tert*-butyl group is larger than that of a trimethylsilyl group, although the former occupies a smaller volume. This is due to the fact that a C−CMe_3 bond is shorter than a C−$SiMe_3$ bond.[25] The presence of rotational isomers in solution, which do not interconvert rapidly on the NMR time scale, is indicated by significantly broadened cyclopentadienyl ^{1}H and ^{13}C{^{1}H} NMR signals.

The molecular structure of the dibromo derivative **4** strongly resembles that of its diiodo homologue.[18] Similar to **3**, the molecule also exhibits an "interlocked" arrangement of the four substituents. When viewed along the axis containing the cyclopentadienyl ring centroids, the order of the substituents of the upper (u) and the lower (l) cyclopentadienyl rings is Me_3C(u)−Br(l)−Br(u)−Me_3C(l). The cyclopentadienyl rings are in a fully eclipsed orientation and essentially coplanar (tilt angle = 1.1°). The two *tert*-butyl groups are bent away from the metal center by 4.8° and 5.1°, respectively.

The conformation of **5** resembles that of fc$(N_3)_2$ in that the N_3 units are almost linear (N−N−N ca. 172°) and aligned in an almost-eclipsed arrangement.[20] The corresponding C_{ipso}−ring centroid−ring centroid−C_{ipso} torsion angle is 12.7°. The N_3 substituents are tilted slightly out of plane from the cyclopentadienyl rings by 8.1° and 6.7°, respectively. The two *tert*-butyl groups are bent away from the metal center by 5.7° and 6.8°, respectively. The cyclopentadienyl rings are very nearly coplanar (tilt angle = 3.1°).

The molecular structure of the cation of [**A′**-**Np**H]BF_4 is very similar to that of its *tert*-butyl-free congener [**A**-**Np**H]BF_4.[8b] The bonding environment of the N atoms is trigonal planar in each case. The N−C−N angle is 131.0(3)°, the C−N bond lengths in this unit are ca. 1.31 Å, and the distance between the formamidinium C atom and the Fe atom is ca. 3.29 Å. The NCN tether causes an essentially eclipsed orientation of the cyclopentadienyl rings (twist angle = 4.2°), together with a pronounced ring tilt of 16.6°. The resulting wedge opens up toward the two *tert*-butyl substituents at the cyclopentadienyl rings. This, in turn, decreases the displacement of the *tert*-butyl substituents out of the cyclopentadienyl ring plane to only 3.7° and 5.6°, respectively.

The presence of the two *tert*-butyl groups in the backbone of **A′**-**Np** is expected to have a negligible influence on the steric environment of the diaminocarbene moiety. In order to probe potential electronic effects of these substituents on the carbene properties, we have determined its TEP value from the IR spectroscopic data of the rhodium(I) carbonyl complex *cis*-[RhCl(**A′**-**Np**)$(CO)_2$], which we prepared via the corresponding 1,5-cyclooctadiene (COD) chelate *cis*-[RhCl(**A′-Np**)(COD)]. We note, in passing, that both rhodium complexes have molecular C_1 symmetry, causing rather complex NMR spectra. For example, because of the chemical inequivalence of the two neopentyl groups, each of them gives rise to a singlet for the $CH_2C(CH_3)_3$ protons and two doublets for the $CH_2C(CH_3)_3$ protons ($|^2J_{HH}| \approx 14$ Hz, AX spin system) in the ^{1}H NMR spectrum. It turns out that the TEP value of **A′-Np** (2050 cm^{-1}, calculated using the linear regression introduced by Dröge and Glorius,[6b] is essentially identical to the TEP values of its *tert*-butyl-free analogues (2049 ± 1 cm^{-1}).

These results indicate that the ligand properties of **A′-Np** are essentially identical to those of its congener **A-Np**. However, this does not necessarily mean that the free carbenes do not differ in terms of chemical reactivity. The exceptional reactivity of **A-Np**, which resembles that of the (alkyl)(amino)carbenes published by Bertrand and co-workers,[26] can be traced back to the ambiphilic nature of this carbene.[10] It has a high-energy lone pair of electrons (high-level HOMO) and a readily accessible vacant orbital (low-level LUMO) at the divalent carbon atom, rendering this carbene highly nucleophilic and electrophilic at the same time.[27] The HOMO and LUMO energies of **A-Np** and **A′-Np** are indeed very similar, according to the results of our DFT calculations (BP86/def2-SVP), and the same holds true for their singlet−triplet gap ΔE_{ST} (see Table 1). ΔE_{ST}, which correlates with the HOMO−LUMO gap,[28] is known to be a reliable indicator of the electrophilicity of a singlet carbene.[29] While Arduengo carbenes have fairly large ΔE_{ST} values (>ca. 70 kcal/mol), more reactive singlet carbenes suitable for small-molecule activation typically have significantly lower ΔE_{ST} values.[10b,26,30]

Table 1. Calculated Frontier Orbital Energies and Adiabatic Singlet−Triplet Gaps (BP86/def2-SVP)

compound	HOMO [eV]	LUMO [eV]	ΔE_{ST} [kcal/mol]
A-Np	−4.04	−0.35	35.2
A′-Np	−3.94	−0.27	35.1

In view of the essentially identical electronic profiles of **A-Np** and **A′-Np**, we expected that **A′-Np** should react with carbon monoxide (CO) under the same mild conditions as **A-Np**, affording a product analogous to the unique betainic enolate (**A-Np**)=C(O$^-$)(**A-Np**$^+$) (Figure 2, *vide supra*). This indeed turned out to be the case. In view of the fact that **A′-Np** is a racemic mixture of the S_p,S_p and R_p,R_p enantiomers, two pairs of enantiomers are possible for this product, viz. (R_pR_p-**A′-Np**)=C(O$^-$)(R_pR_p-**A′-Np**$^+$)/(S_pS_p-**A′-Np**)=C(O$^-$)(S_pS_p-**A′-Np**$^+$) and (R_pR_p-**A′-Np**)=C(O$^-$)(S_pS_p-**A′-Np**$^+$)/(S_pS_p-**A′-Np**)=C(O$^-$)(R_pR_p-**A′-Np**$^+$). The ^{1}H NMR spectrum of the carbonylation product is too complicated to allow for an unambiguous assignment of individual resonance signals to the individual diastereomers. In the case of (**A-Np**)=C(O$^-$)(**A-Np**$^+$), the most conspicuous signals in the ^{1}H NMR spectrum are two low-field doublets located at ca. 4.9 and 5.2 ppm.[10c] This pair of doublets is due to one of the four methylene units present. The signals caused by the other three methylene units are located well below 4.0 ppm, upfield from the cyclopentadienyl region. In the present case, closer inspection of the spectral region from 4.9−5.4 ppm reveals a more complex pattern of overlapping doublets, because of the different diastereomers (Figure 8).

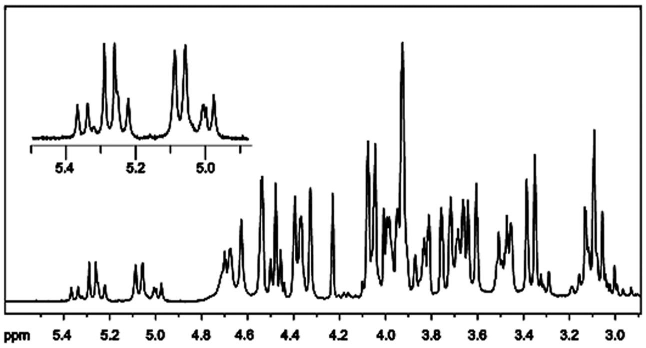

Figure 8. Section of the ^{1}H NMR spectrum of the carbonylation products of **A′-Np** (see Figure S42 in the Supporting Information for the complete spectrum). The inset shows the region characteristic of the low-field CH_2t-Bu signals.

A small amount of crystals could be obtained from a hexane solution of this mixture of isomers after several weeks. After many attempts, one of them was identified to be suitable for a single-crystal XRD study and turned out to contain the enantiomers (R_pR_p-**A′-Np**)=C(O$^-$)(R_pR_p-**A′-Np**$^+$) and (S_pS_p-**A′-Np**)=C(O$^-$)(S_pS_p-**A′-Np**$^+$) as a racemic compound (Figure 9). The remaining crystals were subjected to NMR spectroscopic analysis, which revealed a significantly simplified pattern of well-resolved doublets in the spectral region from 4.9−5.4 ppm, compatible with the presence of only a single diastereomer (see Figure S43 in the Supporting Information). The molecular structure is very similar to that of (**A-Np**)=C(O$^-$)(**A-Np**$^+$).[10c] The C1−C2 and C1−O1 bonds of the enolate-type core (1.362(3) and 1.278(3) Å, respectively) possess partial double-bond character, while the C1−C31 distance of 1.522(3) Å corresponds to a single bond. The cationic charge is delocalized in the formamidinium-like unit containing the atoms N3, C31, and N4. The two N atoms are in a trigonal planar bonding environment (sum of angles: 359.4(2)° for N3, 359.9(2)° for N4). The C−N bond lengths of ca. 1.34 Å and the N−C−N angle of 124.6(2)° deviate

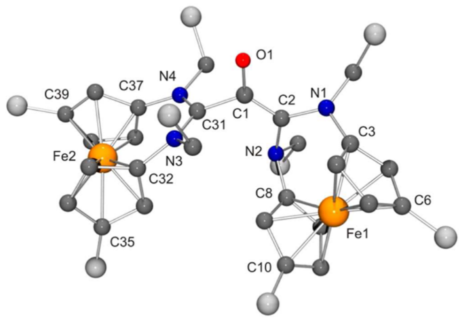

Figure 9. Molecular structure of (R_pR_p-**10**)=C(O$^-$)(R_pR_p-**10**$^+$) in the crystal. The other enantiomer of the racemic compound is not shown. H atoms and methyl C atoms are omitted for clarity, and the quaternary *t*-Bu C atoms are shown as larger circles in lighter gray. Selected bond lengths and bond angles: C1−O1, 1.278(3) Å; C1−C2, 1.362(3) Å; C1−C31, 1.522(3) Å; C2−N1, 1.429(3) Å; C2−N2, 1.464(3) Å; C3−N1, 1.416(3) Å; C8−N2, 1.425(3) Å; C31−N3, 1.348(3) Å; C31−N4, 1.337(3) Å; C32−N3, 1.428(3) Å; C37−N4, and 1.440(3) Å; C2−C1−O1, 129.6(2)°; C2−C1−C31, 118.2(2)°; C31−C1−O1, 112.0(2)°; N1−C2−N2, 119.4(2)°; C2−N1−C3, 116.6(2)°; C2−N2−C8, 113.5(2)°; N3−C31−N4, 124.6(2)°; C31−N3−C32, 124.8(2)°; and C31−N4−C37, 125.4(2)°.

considerably from those of the second unit, which contains C2 and the two pyramidalized nitrogen atoms N1 and N2 (average C−N distance = 1.45 Å, N−C−N angle = 119.4(2)°; sum of angles: 355.8(2)° for N1, 338.8(2)° for N2).

The unusual reactivity of **A′-Np** is further underlined upon closer inspection of a minor side product which was obtained by serendipity from the synthesis of *cis*-[RhCl(**A′-Np**)(COD)]. Standard workup and careful chromatographic purification (dichloromethane eluent) afforded a small amount of the dichloromethane activation product **A′-Np**H−$CHCl_2$, which was structurally characterized by single-crystal XRD (see Figure 10). We have also obtained this compound in a rational synthesis, which revealed that free **A′-Np** indeed reacts smoothly and swiftly with dichloromethane.

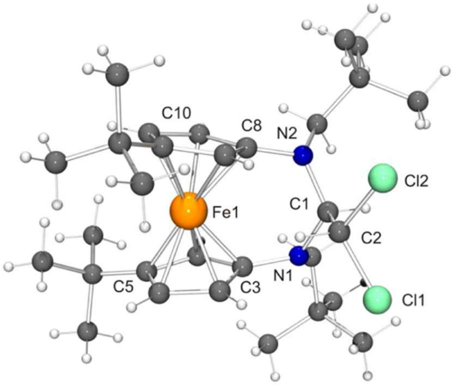

Figure 10. Molecular structure of **A′-Np**H−$CHCl_2$ in the crystal. Selected bond lengths and bond angles: C1−C2, 1.540(3) Å; C1−N1, 1.467(3) Å; C1−N2, 1.471(3) Å; C2−Cl1, 1.782(2) Å; C2−C12, 1.779(2) Å; C3−N1, 1.421(3) Å; and C8−N2, 1.420(3) Å; N1−C1−N2, 117.5(2)°; Cl1−C2−Cl2, 108.5(1)°; C1−N1−C3, 118.4(2)°; C1−N2−C8, 117.0(2)°.

The structure of the fc′ backbone is expected to be affected only marginally by reactions at the carbon atom of the tether. The cyclopentadienyl ring tilt (14.9°) and twist angles (1.5°) of **A′-Np**H−$CHCl_2$ are indeed similar to those of [**A′-Np**H]BF_4. The C−N bond lengths in the NCN unit are typical of $C(sp^3)-N(sp^3)$ single bonds (ca. 1.47 Å),[31] while the formamidinium cation [**A′-Np**H]$^+$ exhibits much shorter bonds (ca. 1.31 Å), because of significant π-delocalization of the positive charge over the NCN unit. In the same vein, the N−C−N angle of **A′-Np**H−$CHCl_2$ is much more acute than that of [**A′-Np**H]$^+$ (117.5(2)° vs 131.0(3)°). The $N_2CH-CHCl_2$ unit is in a fully staggered conformation (H−C−C−H torsion angle = 178.9°). Neither the Cl atoms nor the N atoms are involved in short contacts compatible with hydrogen bonds.

The activation of dichloromethane is unprecedented for NHCs and related diaminocarbenes. In contrast, formal insertion reactions of NHCs with the activated C−H bonds of chloroform and acetonitrile under mild conditions are well-known.[32] A stepwise acid−base reaction mechanism involving the deprotonation of $CHCl_3$ or H_3CCN and subsequent nucleophilic addition of the resulting anion to the protonated carbene has been shown to be unlikely. In the present case, the alternative concerted biphilic C−H activation process seems even more reasonable, since the acidity of dichloromethane is lower than that of chloroform and acetonitrile.[33] The unexpected dichloromethane activation product **A′-Np**H−$CHCl_2$ prompted us to investigate the reactivity of **A-Np** toward dichloromethane, which we had noted merely as a sideline in a previous electrochemical study.[8b] Indeed, this NHC was found to react equally well with CH_2Cl_2, forming the corresponding dichloromethane activation product **A-Np**H−$CHCl_2$ in quantitative yield, according to ^1H NMR spectroscopy. The $N_2CH-CHCl_2$ unit gives rise to two doublets at 4.87 and 6.16 ppm with $^3J_{HH}$ = 9.6 Hz. In the case of **A′-Np**H−$CHCl_2$, these characteristic signals are located at 4.81 and 6.09 ppm. The molecular structure of **A-Np**H−$CHCl_2$, which we determined by a single-crystal XRD study, is similar to that of **A′-Np**H−$CHCl_2$ and also resembles that of the acetonitrile activation product **A-Np**H−CH_2CN (see Figures S1 and S2 in the Supporting Information).

The results presented so far demonstrate that the stable carbenes **A′-Np** and **A-Np** are very similar, in terms of chemical reactivity and ligand properties. However, this may very well be different for the corresponding radical cations **A′-Np**$^{\bullet+}$ and **A-Np**$^{\bullet+}$, the hypothesis being that, in contrast to the delocalized nature of the latter species, **A′-Np**$^{\bullet+}$ will exhibit a more localized ferrocenium-type backbone, together with a less-perturbed diaminocarbene moiety. Electrochemical studies on the free carbene **A′-Np** and its immediate precursors **8**, **9**, and [**A′-Np**H]BF_4, as well as on 1,1′-di-*tert*-butylferrocene (**1**) were performed in order to explore the prospects of isolating and investigating the oxidized carbene **A′-Np**$^{\bullet+}$, as well as to quantify the effect of the electron-donating *tert*-butyl substituents on the redox potentials. Because of the demonstrated reactivity of the free carbene, including that toward dichloromethane (*vide infra*), and in order to provide constant conditions for the investigated compounds, all electrochemical experiments were performed inside a glovebox using a 0.1 M solution of oven-dried NBu_4PF_6 in THF freshly distilled from the blue sodium benzophenone ketyl radical as the supporting electrolyte. Pertinent data are summarized in Table 2.

Table 2. Electrochemical Data for Selected Ferrocene Derivatives of This Study

compound	$E_{1/2}{}^{0/+}$ [V][a]	ΔE_p [mV][a]
1	−0.085	60
8	−0.080	70
9	−0.770[b]	80[b]
[**A′-Np**H]BF_4	+0.300	90
[**A′-Np**H]BF_4	+0.420	89
A′-Np	−0.310	115
A′-Np(H_2O)	−0.437	105
A-Np(H_2O)	−0.418	110

[a] Determined in THF/NBu_4PF_6 (0.1 M) at room temperature and ν = 100 mV/s. [b] A second oxidation was observed at $E_{1/2}$ = +0.395 V.

1,1′-Di-*tert*-butylferrocene (**1**) displays the expected chemically and electrochemically reversible one-electron oxidation at a half-wave potential of −0.085 V vs the ferrocene/ferrocenium couple (see Figure S4 in the Supporting Information). Comparison with the literature data for 1,1′,3,3′-tetra-*tert*-butylferrocene (−0.238 V in CH_3CN/NBu_4ClO_4[34] or −0.250 V in CH_2Cl_2/NBu_4PF_6[35] and for 1,1′,2,2′,4,4′-hexakis-*tert*-butylferrocene (−0.360 V in CH_2Cl_2/NBu_4PF_6,[36] all with respect to $Cp_2Fe^{0/+}$ = 0.000 V), suggests that the inductive effect of a *tert*-butyl substituent on the redox potential of the ferrocene nucleus is only slightly larger than that of a methyl substituent of ca. −54 mV.[37,38] This conclusion is based on the assumption that, in accord with Lever's electrochemical parameter (E_L) approach,[39] the simple additive scheme established for ferrocenes in general, and for the series of methyl-substituted ferrocenes in particular, holds here as well. However, we note that a considerably more negative value of $E_{1/2} = -0.30$ V had previously been reported for 1,1′-di-*tert*-butyl-ferrocene (**1**) in CH_2Cl_2/NBu_4PF_6.[14]

The corresponding diimine **8** oxidizes at a potential that is almost identical to that of **1**, viz. −0.080 V (Figure S5 in the Supporting Information). Reduction of this diimine to the corresponding diamine **9** renders the substituents much stronger electron donors, as is seen by a large cathodic shift of the half-wave potential to −0.770 V (see Figures S6 and S7 in the Supporting Information). The second oxidation of the 1,1′-bis(neopentylamino)-substituted ferrocene **9** at a half-wave potential of +0.395 V also appears to be a chemically and electrochemically reversible process, as judged by square-wave voltammetry (see Figure S8 in the Supporting Information). However, a more stringent analysis is prohibited by the proximity of that wave to the anodic discharge limit of the electrolyte (see Figure S6 in the Supporting Information). Chemically prepared $\mathbf{9}^{\bullet+}$ (oxidation with $[FeCp_2]PF_6$), while EPR silent in a fluid solution at room temperature, displays an axial EPR signal at 103 K with a strongly decreased splitting of the *g*-tensor, when compared to ordinary ferrocenes (see Figure 11; the ferrocenium ions $\mathbf{1}^+$, $\mathbf{8}^+$, and $[\mathbf{A'}\text{-}\mathbf{Np}H]^{2+}$ are EPR silent under these conditions). Thus, the *g*-tensor components were determined as 2.488 ($g_{\parallel}$) and 1.999 ($g_{\perp}$; $\Delta g = 0.489$). This *g* anisotropy is to be compared to that of >3.0 for the ferrocenium ion itself and that of >2.5 for congeners with simple alkyl substituents.[40] While no EPR data on other amino-substituted ferrocenium ions seem to be available, unusually small Δg values have been reported for the *N*-acetylamino-ferrocenium ion ($\Delta g = 1.563$) or for ferrocenium ions $Fc^+{-}NH{-}C({=}O){-}C_6H_3(OH\text{-}2)(\textit{tert}\text{-butyl})_2\text{-}3,5$ with phenol ($\Delta g = 1.665$) or $Fc^+{-}NH{-}C({=}O){-}C_6H_3(O^-\text{-}2)(\textit{tert}\text{-butyl})_2\text{-}3,5$ with phenolato substituents ($\Delta g = 1.192$), the latter exhibiting low-energy excited-state charge transfer from the attached phenolato substituent to the ferrocenium moiety via an N−H···O hydrogen bridge between the amide substituent and the adjacent phenolato oxygen atom.[41] An even smaller Δg value of 0.96 was found for an oxidized ferrocenyl-alkenyl ruthenium conjugate $[Fc{-}CH{=}CH{-}Ru(CO)Cl(P\textit{i}\text{-}Pr_3)_2]^+$ where an estimated 20% of the unipositive charge is delocalized onto the alkenylruthenium moiety.[42] In view of the established correlations between Δg and the charge on the Fe atom[43] the exceedingly low *g* anisotropy of $\mathbf{9}^{\bullet+}$ seems to indicate that the unipositive charge is strongly delocalized onto the amino substituents. This may also explain the negligible effect of the *tert*-butyl substituents on the potential of the first oxidation compared to the counterpart of **9** without *tert*-butyl substituents.[8b]

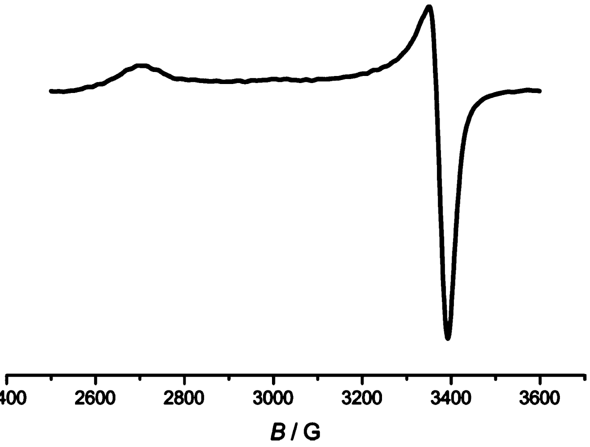

Figure 11. EPR spectrum of $\mathbf{9}^{\bullet+}$ at $T = 103$ K.

$[\mathbf{A'}\text{-}\mathbf{Np}H]BF_4$ is also reversibly oxidized at a half-wave potential of +0.300 V (see Figure S9 in the Supporting Information). To provide a direct comparison to our previous data on $[\mathbf{A}\text{-}\mathbf{Np}H]BF_4$ lacking the *tert*-butyl substituents, the half-wave potential of this compound was also measured in THF/NBu_4PF_6. Its value is +0.420 V, which corresponds to a cathodic shift of 0.120 V caused by two *tert*-butyl substituents.

The most important point of this study is the electrochemical characterization of free carbene **A′-Np**. When freshly prepared **A′-Np** was added to the THF/NBu_4PF_6 supporting electrolyte, a main, reversible one-electron wave at a half-wave potential of −0.437 V, denoted as peaks B/B′ in Figure 12a, was detected. This value is close to those of −0.420 and −0.415 V, which we had previously assigned to **A-Np** and its adamantyl-substituted congener.[8b] What aroused our suspicion, however, was the observation of another wave A/A′ in Figure 12, ca. 0.130 V positive of that couple, whose associated peak currents rapidly decreased on the expense of wave B/B′. When **A′-Np** was added to a filtered THF/NBu_4PF_6 supporting electrolyte prepared from freshly distilled THF after further treatment with KH inside the glovebox, cyclic and square wave voltammetry gave a pattern of two overlapping processes (waves A/A′ and B/B′ in cyclic voltammetry or peaks A and B in square wave voltammetry, respectively) with appreciably higher peak currents for the A/A′ couple (Figure 12b). According to deconvoluted square wave voltammograms, the initial peak current ratio of peak A to that of peak B is ∼4.5:1 (see Figure 12c). When the evolution of the voltammograms was monitored over time, a gradual decrease of the A/A′ couple with a concomitant increase of the B/B′ couple was observed, albeit at a much slower rate than observed in the initial experiment without KH pretreatment of the supporting electrolyte.

All these observations let us conclude that wave A/A′ (peak A) corresponds to the redox process of the free carbene **A′-Np** and that this species cleanly converts to a follow-up product, giving rise to the couple B/B′ (peak B). The reaction is slowed considerably after even more rigorous drying of the solvent, which points to water as the reaction partner. In fact, the free carbenes **A-Np** and **A′-Np** react rapidly with water, affording the respective addition product **A-Np**(H_2O) and **A′-Np**(H_2O). We have exemplarily scrutinized the reaction of **A-Np** with a slight excess of water and found that the carbene is instantaneously hydrolyzed to **A-Np**(H_2O) in the form of two isomers, which are in a solvent-dependent equilibrium with each other. The ratio of the major component to the minor component is ca. 5:1 in CD_2Cl_2, 4:1 in THF-d_8, and 3:1 in C_6D_6. Not unexpectedly, the NMR spectra show no indication for the presence of the formal primary water addition product containing a NpN−CH(OH)−NNp unit and are fully in accord with the corresponding ring-opened isomer 1-neopentylformamido-1′-neopentylaminoferrocene $[Fe\{\eta^5\text{-}C_5H_4[NNp(CHO)]\}\{\eta^5\text{-}C_5H_4(NHNp)\}]$,[44] which is expected to give rise to two conformers (*E* and *Z*) of similar energy due

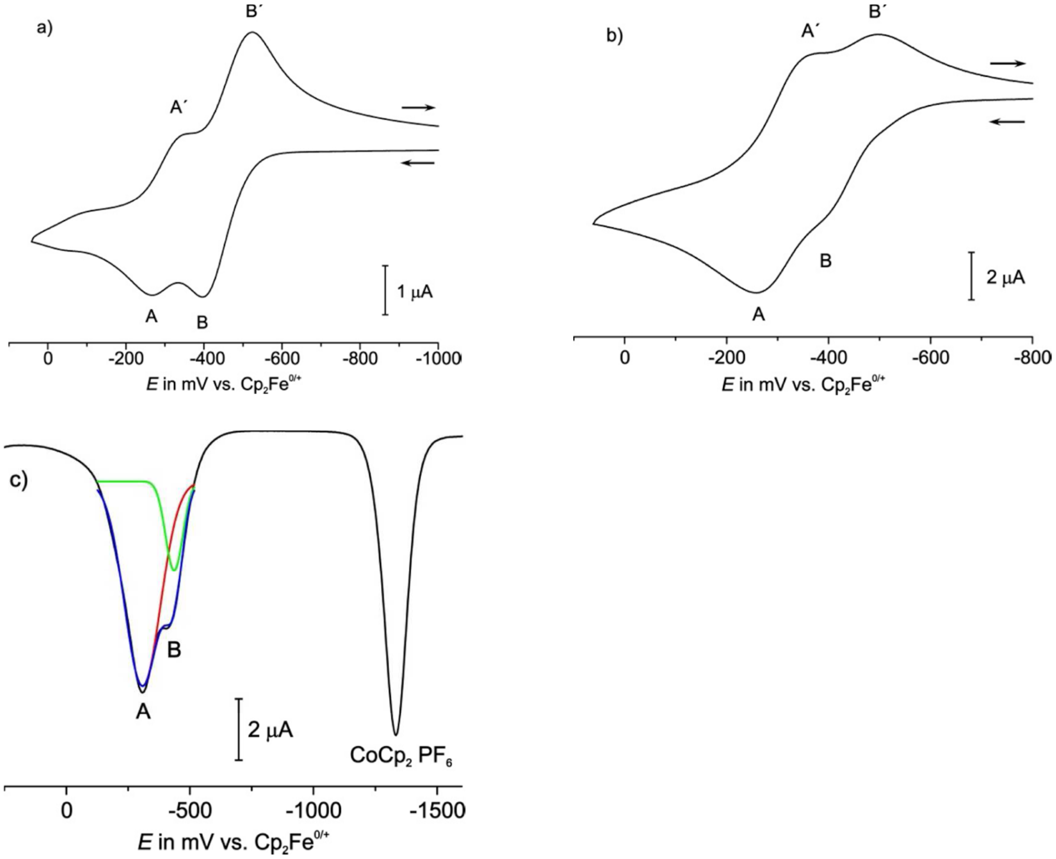

Figure 12. (a) CV of **A′-Np** in 0.1 M THF/NBu_4PF_6 at ν = 100 mV/s (no pretreatment of the supporting electrolyte with KH); (b) CV of **A′-Np** in 0.1 M THF/NBu_4PF_6 at ν = 100 mV/s using supporting electrolyte treated with KH prior to the measurement; (c) square wave voltammogram of **A′-Np** in 0.1 M THF/NBu_4PF_6 with deconvoluted peaks under the same conditions as in panel b.

to the partial double-bond character of the amide C(O)−N bond (Figure 13).[45,46]

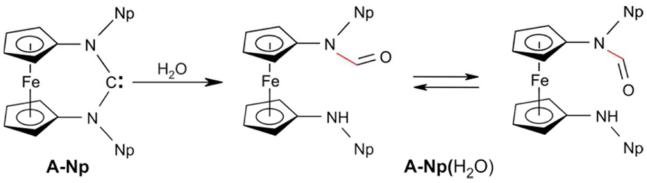

Figure 13. Hydrolysis of **A-Np** to **A-Np**(H_2O), which consists of the conformers (*E*)-[Fe{η^5-C_5H_4[NNp(CHO)]}{η^5-C_5H_4(NHNp)}] (middle) and (*Z*)-[Fe{η^5-C_5H_4[NNp(CHO)]}{η^5-C_5H_4(NHNp)}] (right), according to NMR spectroscopic analysis. The partial double-bond character of the C(O)−N bond responsible for hindered rotation is indicated in red.

In fact, the *E* conformer could be structurally characterized by single-crystal XRD (see Figure S3 in the Supporting Information). The cyclic voltammogram of **A-Np**(H_2O) (see Figure S10 in the Supporting Information) exhibits a reversible one-electron wave at a half-wave potential of −0.418 V (0.1 M THF/NBu_4PF_6), indistinguishable within experimental error from the value of −0.42 V, which we had previously reported for the carbene **A-Np** under these conditions. We note here that the presence of only one redox wave for the two isomers might be either due to a fortuitous identity of the redox potentials of both isomers or to an isomerization rate faster than that of the electrochemical process. This, in essence, means that our previously reported electrochemical data on **A-Np** and its 2-adamantyl analogue **A-Ad** (compounds **2d** and **2c**, respectively, in ref 8b) are incorrect and correspond to the respective hydrolysis product. Because of the less-than-ideal experimental conditions that were available to us at that time and the then-unknown extreme reactivity of the free carbenes, the rapid and quantitative follow-up reaction with adventitious water went unnoticed. Oxidized samples of the hydrolyzed carbene **A-Np**(H_2O) display two closely spaced axial EPR signals, with $g_{\parallel}$ = 2.651 and $g_{\perp}$ = 1.993 (Δg = 0.658) and $g_{\parallel}$ = 2.543 and $g_{\perp}$ = 1.924 (Δg = 0.619), which we assign to the two different isomers (see Figure S11 in the Supporting Information). In keeping with the replacement of an amine by a less electron-donating amide substituent at one of the cyclopentadienyl rings, the *g*-tensor anisotropy of these radical cations is noticeably larger than that of $\mathbf{9}^{\bullet+}$.

■ CONCLUSION

The unusual chemical properties of the ferrocene-based NHC **A-Np**, which we reported in previous studies,[8b,10c] have prompted us to attach two *tert*-butyl groups at the 3,3′-positions of the ferrocenediyl backbone, leading to the title compound **A′-Np**. The *tert*-butyl groups have two major effects. First, they significantly enhance the solubility of the carbene and its precursor compounds in aprotic organic solvents. Second, they cause planar chirality. This latter aspect has not been in the focus of our present investigation, where we have exclusively worked with racemic compounds. Note, however, that chiral resolution should be easily possible at the stage of the immediate carbene precursor, viz. the formamidinium salt, by using a chiral anion.[47] Our main reason for introducing the two *tert*-butyl groups had been to increase the electron density of the ferrocenylene unit to an extent that a one-electron oxidation affords a ferrocenium-type backbone and an essentially unperturbed carbene moiety. The choice of substituents was guided by the report that the oxidation of 1,1′-di-*tert*-butylferrocene (**1**) is easier (by 0.30 V) than that of pristine ferrocene.[14] In our present system, however, the electronic effect of the two *tert*-butyl substituents turned out to be disappointingly low. Apart from this somewhat sobering observation, our investigation has allowed us to recognize that we had underestimated the reactivity of **A-Np** in our previous electrochemical study, where its rapid and quantitative follow-up reaction with adventitious water had gone unnoticed. We now provide clear evidence that the electrochemical data that we reported for **A-Np** and its 2-adamantyl congener **A-Ad** were due to the products of hydrolysis. The astounding reactivity of such ferrocene-based carbenes is also reflected by the fact that **A-Np** and **A′-Np** readily add dichloromethane, which is a reaction that is unprecedented for diaminocarbenes.

We will continue our efforts to make the ferrocene-based carbene backbone of **A-Np** and its congeners considerably more electron-rich (for example, via the introduction of up to eight methyl substituents), and we will report on our findings in due course.

■ EXPERIMENTAL SECTION

General Considerations. All reactions were performed in an inert atmosphere (argon or dinitrogen) by using standard Schlenk techniques or a conventional glovebox. A Hettich ROTINA 46 RS centrifuge suitable for Schlenk tubes was used to separate precipitates that could not easily be removed by filtration. Starting materials were procured from standard commercial sources and used as received. LDA was prepared by reaction of *n*-butyllithium with diisopropylamine at room temperature in hexane, isolated by filtration and dried *in vacuo*. NMR spectra were recorded with Varian NMRS-500 and MR-400 spectrometers operating at 500 and 400 MHz, respectively, for ^{1}H. Where necessary, signal assignments were made with the help of 2D NMR experiments, in particular HSQC, HMBC, and HH−COSY. High-resolution ESI mass spectra were obtained with a micrOTOF time-of-flight mass spectrometer (Bruker Daltonics, Bremen, Germany) using an Apollo "ion funnel" ESI source. Mass calibration was performed immediately prior to the measurement with ESI Tune Mix Standard (Agilent, Waldbronn, Germany). IR spectra were recorded with a Bruker ALPHA FT-IR spectrometer. Elemental analyses were carried out with a HEKAtech Euro EA-CHNS elemental analyzer at the Institute of Chemistry, University of Kassel, Germany. All electrochemical experiments were executed in a home-built cylindrical vacuum-tight one-compartment cell at room temperature inside a Vacuum Atmospheres glovebox. A spiral-shaped Pt wire and a Ag wire served as the counter and pseudo-reference electrodes. A platinum electrode is introduced as the working electrode through the top port via a Teflon screw cap with a suitable fitting. It was polished with first 1 μm and then 0.25 μm diamond paste before measurements. The cell allows experiments to be performed with ~5 mL of analyte solution. NBu_4PF_6 (0.1 M) in THF was used as the supporting electrolyte. Referencing was done with addition of an appropriate amount of cobaltocenium hexafluorophosphate or decamethylferrocene ($Cp*_2Fe$) as an internal standard to the analyte solution after all data of interest had been acquired. Representative sets of scans were repeated with the added standard. Final referencing was done against the ferrocene/ferrocenium ($Cp_2Fe^{0/+}$) couple with $E_{1/2}$ $Cp_2Co^{0/+}$ = −1.344 V vs $Cp_2Fe^{0/+}$ or $E_{1/2}$ $Cp*_2Fe^{0/+}$ = −0.540 V vs $Cp_2Fe^{0/+}$ under our conditions. Electrochemical data were acquired with a computer-controlled BAS CV50 potentiostat. Electron paramagnetic resonance (EPR) studies were performed on a table-top X-band spectrometer (Model MiniScope MS 400, Magnettec).

Preparative Work. *tert-Butylcyclopentadiene.* Freshly distilled cyclopentadiene (33.1 g, 501 mmol) was added over a period of 5 min to a vigorously stirred solution of KO*t*-Bu (59.0 g, 526 mmol) in THF (250 mL) cooled in an ice bath. A thick yellowish suspension resulted which was brought to reflux, affording a yellow solution to which *t*-BuBr (75.4 g, 550 mmol) was added dropwise over a period of 1 h. Slow formation of a colorless precipitate accompanied by sluggish gas evolution was observed. The reaction mixture was refluxed for a further 1 h and subsequently allowed to cool to room temperature. The following workup was performed under aerobic conditions. The precipitate was filtered off with suction and washed with hexane (4 × 100 mL). The filtrate and washings were combined. Volatile components were removed using a rotary evaporator (60 °C bath temperature, final pressure 300 mbar). The brownish yellow residue was subjected to rapid bulb-to-bulb distillation under inert atmosphere affording *tert*-butylcyclopentadiene as a colorless liquid. The product is a mixture of two isomers (ratio ca. 1:2).[48] It turned out to be slightly contaminated with THF (ca. 5%), which was conveniently quantified by ^{1}H NMR spectroscopy. The crude product was used without further purification for the synthesis of **1**. Yield: 27.0 g (45%). Major isomer: ^{1}H NMR ($CDCl_3$): δ = 1.18 (s, 9H, CMe_3), 2.95 (m, 2H, CH_2), 5.98, 6.43 6.62 (3 m, 3 × 1H, CH). $^{13}C\{^1H\}$ NMR ($CDCl_3$): δ = 29.8 (CMe_3), 32.1 (CMe_3), 40.9 (CH_2), 122.4, 132.0, 133.5 (3 × CH), 159.8 ($CCMe_3$). Minor isomer: δ = 1.19 (s, 9H, CMe_3), 2.95 (m, 2H, CH_2), 6.17, 6.27, 6.42 (3 m, 3 × 1H, CH). $^{13}C\{^1H\}$ NMR ($CDCl_3$): δ =31.0 (CMe_3), 33.2 (CMe_3), 40.1 (CH_2), 123.5, 130.4, 132.8 (3 × CH), 156.9 ($CCMe_3$).

*1,1′-Di-tert-butylferrocene (**1**).* A solution of *n*-BuLi in hexane (70.0 mL, 1.60 M, 112 mmol) was added over a period of 15 min to a stirred solution of crude *tert*-butylcyclopentadiene (14.5 g, purity ca. 95%, ca. 113 mmol) in THF (200 mL) cooled in an ice bath. After 10 min, $FeCl_2$ (7.00 g, 55.2 mmol) was added. The ice bath was replaced by an oil bath and the mixture refluxed for 14 h. Volatile components were removed *in vacuo*. Hexane (100 mL) was added to the residue. The resulting suspension was filtered through a pad of silica gel. Volatile components were removed from the filtrate *in vacuo*, leaving the product as a dark orange oil that was sufficiently pure (>95%) for the next step. Yield: 14.7 g (89%). NMR spectroscopic data were fully in accord with those published by Manners and co-workers.[14]

*[(**2**)$_3$(TMEDA)$_2$].* **1** (10.6 g, 35.5 mmol) was dissolved in a solution of *n*-BuLi in hexane (45 mL, 1.60 M, 72.0 mmol). The solution was cooled with an ice bath and TMEDA (3.50 g, 30.1 mmol) was added. The ice bath was removed and the mixture stirred for 2 d. The initially former colorless precipitate (most likely $[(n\text{-BuLi})_4(\text{TMEDA})]_n$)[49] gradually dissolved with concomitant formation of a bright orange powdery solid, which was filtered off, washed with hexane (3 × 20 mL), and dried *in vacuo*. Yield: 9.56 g (70%). The compound is almost insoluble in aromatic solvents and diethyl ether. It decomposes rapidly in THF. A **2**:TMEDA ratio of 3:2 was determined gravimetrically upon reaction with an excess of chlorotrimethylsilane in diethyl ether (*vide infra*). **1** can easily be recovered from the combined mother liquor and washings by careful quenching with ethanol at 0 °C until the initially forming suspension completely dissolves, followed by standard aqueous acidic workup and chromatographic purification (silica gel, hexane), affording 2.90 g (27%) of recovered starting material.

*rac-fc′(SiMe$_3$)$_2$ (**3**).* [(**2**)$_3$(TMEDA)$_2$] (512 mg, 0.44 mmol ≡ 1.32 mmol of **2**) was added to a stirred solution of chlorotrimethylsilane (430 mg, 3.96 mmol) in diethyl ether (20 mL) kept at −20 °C. A dark brown suspension formed, which was allowed to warm to room temperature and stirred for an additional 30 min. Volatile components were removed *in vacuo*. Hexane (20 mL) was added to the residue. Insoluble material was removed by filtration through a short pad of Celite and washed with hexane (3 × 2 mL). Volatile components were removed from the combined filtrate and washings, affording **3** in high purity, as shown by ^{1}H NMR spectroscopy. Yield: 576 mg (98%). Mp: 144 °C. Crystals suitable for a single-crystal XRD study were obtained by crystallization from hexane at −20 °C.

^{1}H NMR (C_6D_6): δ = 0.30 (s, 18H, $SiMe_3$), 1.25 (s, 18H, CMe_3), 4.06, 4.08, 4.17 (3 br.s, 3 × 2H, CH). $^{13}C\{^1H\}$ NMR (C_6D_6): δ = 0.9

($SiMe_3$), 31.0 (CMe_3), 32.2 (CMe_3), 68.1, 70.8 (2 × CH), 70.7 ($CSiMe_3$), 73.6 (br., CH), 104.3 ($CCMe_3$). HRMS/ESI(+): m/z = 442.2154 $[M]^+$; 442.2174 calcd for $[C_{24}H_{42}FeSi_2]^+$.

Anal. Calcd for $C_{24}H_{42}FeSi_2$ (442.62): C, 65.13; H, 9.56. Found: C, 65.27; H, 9.90.

rac-fc′Br₂ **(4)**. **1** (1.19 g, 3.99 mmol) was dissolved in a solution of *n*-BuLi in hexane (5.1 mL, 1.60 M in hexane, 8.16 mmol). The reaction mixture was cooled with an ice bath. TMEDA (948 mg, 8.16 mmol) was added and the mixture stirred at room temperature for 2 d, affording a bright orange suspension. Diethyl ether (10 mL) was added and the mixture cooled to −78 °C. A solution of 1,1,2,2-tetrabromoethane (2.82 g, 8.16 mmol) in diethyl ether (2 mL) was added dropwise. The reaction mixture was stirred for 10 min and subsequently allowed to warm to room temperature during the course of 2.5 h, affording a deep red solution with a colorless precipitate. The product was isolated by standard aqueous work up, followed by flash chromatography (silica gel, diethyl ether) to remove some dark, polar impurities. The resulting bright yellow solution was dried with sodium sulfate, which was subsequently removed by filtration. Volatile components were removed from the filtrate *in vacuo*. The residue was dissolved in a minimal amount of diethyl ether and crystallized at −20 °C, affording the product as bright yellow crystals. Crystals suitable for a single-crystal XRD were taken from this batch. Yield: 1.13 g (62%). Mp: 72 °C.

^1H NMR (C_6D_6): δ = 1.09 (s, 18H, CMe_3), 3.59, 4.03, 4.25 (3 m, 3 × 2H, CH). $^{13}C\{^1H\}$ NMR (C_6D_6): δ = 30.6 (CMe_3), 31.5 (CMe_3), 66.4, 71.0, 73.5 (3 × CH), 78.7 (CBr), 102.7 ($CCMe_3$). HRMS/ESI(+): m/z = 453.9592 $[M]^+$; 453.9594 calcd for $[C_{18}H_{24}Br_2Fe]^+$.

Anal. Calcd for $C_{18}H_{24}Br_2Fe$ (456.04): C, 47.41; H, 5.30. Found: C, 47.05; H, 5.43.

rac-fc′(N₃)₂ **(5)**. *Caution: The product is very light-sensitive. The following procedure must be carried out with the exclusion of light. Although we have experienced no incidents, we strongly advise performing the procedure behind a safety shield and using the crude product immediately for the next step. Further purification, if at all necessary, as well as melting point determination, should be performed on the smallest scale possible.* ($\mathbf{2}$)$_3$(TMEDA)$_2$ (5.00 g, 4.3 mmol ≡ 12.9 mmol of **2**) was added over a period of 5 min to a stirred solution of tosyl azide (5.01 g, 25.4 mmol) in diethyl ether (50 mL) cooled to −30 °C. After 15 min, the stirred mixture was brought to room temperature by means of a water bath and stirred for an additional hour. The water bath was replaced by an ice bath and the reaction was quenched via careful addition of ice-cold water (3.0 mL), affording a burgundy red solution. After ca. 15 min, a colorless precipitate started to form. The suspension was stirred for an additional 45 min. The deep yellow supernatant was separated by decanting. The residue was extracted with diethyl ether (4 × 5 mL), and the extracts were separated by decanting. The combined supernatant and extracts were dried with potassium carbonate, which was subsequently removed by filtration. Volatile components were removed *in vacuo*, leaving the product as an orange solid, which was slightly contaminated with unreacted tosyl azide (ca. 3%), according to ^1H NMR spectroscopy. The crude product was immediately used for the next step without further purification. An analytically pure sample was obtained by recrystallization from acetonitrile, which also afforded crystals suitable for a single-crystal XRD study. Yield: 4.70 g (96%). Mp: 51 °C.

^1H NMR ($CDCl_3$): δ = 1.22 (s, 18H, CMe_3), 3.90, 4.26, 4.28 (3 m, 3 × 2H, CH). $^{13}C\{^1H\}$ NMR ($CDCl_3$): δ = 30.5 (CMe_3), 31.4 (CMe_3), 59.2, 60.4, 63.3 (3 × CH), 99.2 (CN), 100.1 ($CCMe_3$). HRMS/ESI(+): m/z = 380.1407 $[M]^+$; 380.1412 calcd for $[C_{18}H_{24}FeN_6]^+$.

Anal. Calcd for $C_{18}H_{24}FeN_6$ (380.28): C, 56.85; H, 6.36; N, 22.10. Found: C, 56.76; H, 6.63; N, 21.03.

rac-fc′(NH₂)₂ **(6)**. Methanol (20 mL) was added to **5** (3.20 g, 8.41 mmol) and Pd/C (0.45 g, 10% Pd, ca. 5 mol %). The nitrogen atmosphere was replaced by hydrogen. The reaction mixture was stirred vigorously under a slight flow of H_2. A mildly exothermic reaction ensued, which was controlled by cooling with a water bath from time to time. The starting material dissolved completely during the reaction. After 1 h, the hydrogen atmosphere was replaced by a nitrogen atmosphere. The catalyst was removed by filtration through a Celite pad, affording a yellow solution. Volatile components were removed *in vacuo*, leaving the crude product as a very air-sensitive brownish orange residue, which slowly solidified to a glassy mass. Yield: 2.62 g (95%). Mp: 122 °C. An analytically pure sample was obtained by crystallization from acetonitrile at −20 °C.

^1H NMR (C_6D_6): δ = 1.24 (s, 18H, CMe_3), 1.93 (br.s, 2H, NH_2), 3.45, 3.59, 3.68 (3 m, 3 × 2H, CH). $^{13}C\{^1H\}$ NMR (C_6D_6): δ = 30.8 (CMe_3), 31.9 (CMe_3), 58.5, 59.1, 61.9 (3 × CH), 97.2 ($CCMe_3$), 102.9 (CN) ppm. HRMS/ESI(+): m/z = 328.1615 $[M]^+$; 328.1602 calcd for $[C_{18}H_{28}FeN_2]^+$.

Anal. Calcd for $C_{18}H_{28}FeN_2$ (328.28): C, 65.86; H, 8.60; N, 8.53. Found: C, 66.71; H, 8.47; N, 8.58.

rac-fc′(NHBoc)₂ **(7)**. Methanol (50 mL) was added to **5** (4.61 g, 12.1 mmol) and Pd/C (0.67 g, 10% Pd, ca. 5 mol %). The nitrogen atmosphere was replaced by hydrogen. The reaction mixture was stirred vigorously under a slight flow of H_2. A mildly exothermic reaction ensued, which was controlled by cooling with a water bath from time to time. The starting material dissolved completely during the reaction. After 1 h, the hydrogen atmosphere was replaced by a nitrogen atmosphere. Di-*tert*-butyl dicarbonate (5.46 g, 25.0 mmol) was added to the stirred mixture, whereupon a mildly exothermic reaction with slow gas evolution (CO_2) was observed. The reaction mixture was stirred for 15 h and subsequently filtered through a Celite pad to remove the catalyst. Analysis of an aliquot of the reaction mixture by ^1H NMR spectroscopy confirmed complete conversion at this point. This solution can be used for the synthesis of $[\mathbf{6}H_2]Cl_2$ without further workup (*vide infra*). The following workup was performed under aerobic conditions. Volatile components were removed *in vacuo*, including residual amounts of di-*tert*-butyl dicarbonate, which were finally sublimed off at 50 °C (cooling finger temperature = −30 °C). Yield: 6.13 g (92%). Mp: 157−158 °C. Optional additional purification can be performed by column chromatography (silica gel, hexane/Et_2O = 5:1), affording a pale yellow microcrystalline solid of analytical purity.

^1H NMR (C_6D_6): δ = 1.21 (s, 18H, $CCMe_3$), 1.48 (s, 18H, $OCMe_3$), 3.78 (s, 2H, CH), 4.00, 4.61 (2 br.s, 2 × 2H, CH), 6.51 (br.s, 2H, NH). $^{13}C\{^1H\}$ NMR (C_6D_6): δ = 28.5 ($CCMe_3$), 30.6 ($OCMe_3$), 31.7 ($CCMe_3$), 61.1, 61.6, 62.9 (3 × br., CH), 79.4 (br., $OCMe_3$), 95.8 (cyclopentadienyl CN), 98.6 ($CCMe_3$), 154.2 (br., C(O)NH). HRMS/ESI(+): m/z = 528.2645 $[M]^+$; 528.2651 calcd for $[C_{28}H_{44}FeN_2O_4]^+$.

Anal. Calcd for $C_{28}H_{44}FeN_2O_4$ (528.52): C, 63.63; H, 8.39; N, 5.30. Found: C, 63.63; H, 8.78; N, 5.18.

[6H₂]Cl₂. The solution of **7** obtained after removal of the catalyst by filtration (*vide supra*) was cooled with an ice bath. Acetyl chloride (5.50 g, 70.0 mmol) was added dropwise over a period of 5 min to the stirred solution. The ice bath was removed and the mixture stirred at room temperature. Slight gas evolution was observed. After 1 h, the temperature was increased to 40 °C and stirring continued until gas evolution had stopped completely (ca. 1 h). The volume of the reaction mixture was reduced to ca. 30 mL *in vacuo*, whereupon crystallization started. Diethyl ether (150 mL) was added over a period of 0.5 h. The bright yellow precipitate was collected by filtration, washed with diethyl ether (2 × 10 mL), and dried *in vacuo*. Yield: 4.04 g (83%, with respect to **5**; 78%, with respect to $[(\mathbf{2})_3(TMEDA)_2]$). Dec. >150 °C.

^1H NMR (DMSO-d_6): δ = 1.18 (s, 18H, CMe_3), 4.20, 4.49, 4.52 (3 m, 3 × 2H, CH), 10.10 (br.s, 6H, NH_3^+). $^{13}C\{^1H\}$ NMR (DMSO-d_6): δ = 30.0 (CMe_3), 31.1 (CMe_3), 61.8, 64.1, 64.6 (3 × CH), 87.6 (CN), 101.0 ($CCMe_3$).

Anal. Calcd for $C_{18}H_{30}Cl_2FeN_2$ (401.20): C, 53.89; H, 7.54; N, 6.98. Found: C, 54.13; H, 7.63; N, 6.68.

rac-fc′(NH=CHtBu)₂ **(8)**. Triethylamine (730 mg, 7.21 mmol) was added to a stirred mixture of $[\mathbf{6}H_2]Cl_2$ (820 mg, 2.04 mmol) and pivalaldehyde (551 mg, 6.40 mmol) in acetonitrile (10 mL). A crystalline precipitate of triethylammonium chloride formed immediately and the yellow suspension gradually darkened. After 3 d, volatile components were removed *in vacuo* (final heating bath temperature = 50 °C). The residue was extracted with hexane (20 mL). The extract

DOI: 10.1021/acs.inorgchem.5b01064
Inorg. Chem. 2015, 54, 6657−6670

was filtered through a short Celite pad and the filtrate reduced to dryness *in vacuo*, affording the product as a dark orange microcrystalline solid. Yield: 875 mg (92%).

^{1}H NMR ($CDCl_3$): δ = 1.14 (s, 18H, N=CHC*Me*$_3$), 1.23 (s, 18H, cyclopentadienyl CCMe$_3$), 3.82, 3.92, 4.34 (3 m, 3 × 2H, cyclopentadienyl CH), 8.00 (s, 2H, N=CH). ^{13}C{^{1}H} NMR ($CDCl_3$): δ = 26.9 (N=CHC*Me*$_3$), 30.6 (cyclopentadienyl C*C*Me$_3$), 31.5 (cyclopentadienyl CC*Me*$_3$), 36.8 (N=CH*C*Me$_3$), 61.8, 64.0, 65.1 (3 × cyclopentadienyl CH), 101.2 (cyclopentadienyl *C*CMe$_3$), 104.8 (cyclopentadienyl CN), 170.1 (N=*C*HCMe$_3$). HRMS/ESI(+): *m*/*z* = 465.2937 [M]$^+$; 464.2854 calcd for [$C_{28}H_{44}FeN_2$]$^+$.

Anal. Calcd for $C_{28}H_{44}FeN_2$ (464.52): C, 72.40; H, 9.55; N, 6.03. Found: C, 72.24; H, 10.27; N, 6.11.

rac-fc′(NHNp)$_2$ (9). LiAlH$_4$ (300 mg, 7.91 mmol) was added to a stirred solution of **8** (320 mg, 0.69 mmol) in diethyl ether (4 mL). After 1 h, the mixture was diluted with diethyl ether (10 mL) and cooled with an ice bath. The reaction was quenched via the dropwise addition of ethyl acetate (10.0 mmol, 881 mg), followed by water (570 mg, 31.6 mmol). The mixture was allowed to warm up to room temperature. Insoluble material was separated off by centrifugation. The solid residue was suspended in diethyl ether (10 mL) and subsequently separated off by centrifugation. This extraction procedure was repeated two more times. The combined supernatants were dried with sodium sulfate, which was subsequently removed by filtration. Volatile components were removed from the filtrate *in vacuo*, leaving the product as an orange red microcrystalline solid. Yield: 299 mg (93%). An analytically pure sample was obtained by recrystallization from methanol. Mp: 116−117 °C.

^{1}H NMR (C_6D_6): δ = 0.94 (s, 18H, CH$_2$C*Me*$_3$), 1.29 (s, 18H, cyclopentadienyl CCMe$_3$), 2.21 (t, $^{3}J_{HH}$ = 7.1 Hz, 2H, NH), 2.74 (dd, $^{2}J_{HH}$ = 6.3 Hz, $^{3}J_{HH}$ = 7.1 Hz, 4H, C*H*$_2$CMe$_3$), 3.71, 3.77, 3.79 (3 m, 3 × 2H, CH). ^{13}C{^{1}H} NMR (C_6D_6): δ = 27.9 (CH$_2$C*Me*$_3$), 31.0 (cyclopentadienyl C*C*Me$_3$), 31.6 (CH$_2$*C*Me$_3$), 32.0 (cyclopentadienyl CC*Me*$_3$), 54.7, 56.0, 59.7 (3 × CH), 59.9 (CH$_2$), 96.4 (cyclopentadienyl *C*CMe$_3$), 111.0 (cyclopentadienyl CN). HRMS/ESI(+): *m*/*z* = 468.3165 [M]$^+$; 468.3167 calcd for [$C_{28}H_{48}FeN_2$]$^+$.

Anal. Calcd for $C_{28}H_{48}FeN_2$ (468.55): C, 71.78; H, 10.33; N, 5.98. Found: C, 72.05; H, 10.31; N, 5.94.

[A′-NpH]BF$_4$. A mixture of **9** (1.31 g, 2.80 mmol), ammonium tetrafluoroborate (1.00 g, 9.54 mmol), and triethyl orthoformate (10 mL, ca. 60 mmol) was placed in a preheated oil bath (105 °C) and stirred vigorously for 1 h under reflux conditions. The dark brown mixture was allowed to cool to room temperature. Volatile components were removed *in vacuo*. The residue was taken up in dichloromethane (10 mL). Filtration through a short pad of Celite afforded a clear brown solution. The filtrate was reduced to dryness *in vacuo*. The residue was triturated with diethyl ether (10 mL) under sonication. The yellow solid of composition [**A′-Np**H]BF$_4$·$^1/_2$Et$_2$O (according to ^{1}H NMR spectroscopic analysis) formed was collected by filtration, washed with diethyl ether (2 × 3 mL), and briefly dried *in vacuo*. Yield: 870 mg (52%). Repeated removal of volatile components *in vacuo* from a toluene solution of the product, followed by crystallization afforded crystals which were suitable for an XRD study. Extensive drying *in vacuo* at ca. 50 °C afforded a solvent-free material of analytical purity.

^{1}H NMR (C_6D_6): δ = 1.03 (s, 18H, CH$_2$C*Me*$_3$), 1.08 (s, 18H, cyclopentadienyl CCMe$_3$), 3.94 (m, 2H, CH), 4.00 (s, 4H, C*H*$_2$CMe$_3$), 4.58, 4.65 (2 m, 2 × 2H,CH), 8.78 (s, 1H, N$_2$CH). ^{13}C{^{1}H} NMR (C_6D_6): δ = 28.0 (CH$_2$C*Me*$_3$), 30.2 (cyclopentadienyl C*C*Me$_3$), 31.7 (cyclopentadienyl CC*Me*$_3$), 33.0 (CH$_2$*C*Me$_3$), 66.2, 67.0 (2 × cyclopentadienyl CH), 69.7 (*C*H$_2$CMe$_3$), 71.2 (cyclopentadienyl CH), 95.1 (cyclopentadienyl CN), 105.7 (cyclopentadienyl *C*CMe$_3$), 165.9 (N$_2$CH). HRMS/ESI(+): *m*/*z* = 479.3088 [**A′-Np**H]$^+$; 479.3089 calcd for [$C_{29}H_{47}FeN_2$]$^+$.

Anal. Calcd for $C_{29}H_{47}BF_4FeN_2$ (566.36): C, 61.50; H, 8.37; N, 4.95. Found: C, 61.37; H, 8.62; N, 5.04.

A′-Np. Diethyl ether (5 mL) was added to [**A′-Np**H]BF$_4$ (255 mg, 0.45 mmol) and LDA (51 mg, 0.48 mmol). The mixture was stirred for 15 min. Subsequently, volatile components were removed *in vacuo*. Hexane (10 mL) was added to the residue. Insoluble material was removed by filtration through a short Celite pad. Volatile components were removed from the filtrate *in vacuo*, affording the product as orange viscous oil, which slowly turned to a waxy solid, but refused to crystallize. Yield: 179 mg (83%). The compound is highly soluble in all common aprotic solvents. Because of the noncrystalline consistency and extremely high reactivity of this carbene, we have not been able to obtain satisfactory microanalytical data.

^{1}H NMR (C_6D_6): δ = 1.12, 1.13 (2 s, 2 × 18H, CMe$_3$), 3.89 (m, 4H, CH), 3.92 (m, 2H, CH), 3.95 (s, 4H, CH$_2$). ^{13}C{^{1}H} NMR (C_6D_6): δ = 29.1 (CH$_2$C*Me*$_3$), 30.2 (cyclopentadienyl C*C*Me$_3$), 32.0 (cyclopentadienyl CC*Me*$_3$), 33.6 (CH$_2$*C*Me$_3$), 65.1, 66.2, 67.4 (3 × CH), 73.4 (*C*H$_2$CMe$_3$), 102.8 (cyclopentadienyl CN), 103.4 (cyclopentadienyl *C*CMe$_3$), 267.0 (carbene C).

cis-[RhCl(A′-Np)(COD)]. [{Rh(μ-Cl)(COD)}$_2$] (61 mg, 0.12 mmol) was added to a solution of **A′-Np** (120 mg, 0.25 mmol) in THF (2.5 mL). The reaction mixture was stirred for 2 h. Volatile components were subsequently removed *in vacuo*, leaving a glassy yellow solid. The crude product was subjected to purification by column chromatography (silica gel, dichloromethane), affording an air-stable deep yellow microcrystalline solid. Yield: 108 mg (60%). An analytical sample was obtained by repeated recrystallization from methanol. In addition, chromatographic purification using dichloromethane as eluent serendipitously furnished a few crystals of the dichloromethane activation product **A′-Np**H−CHCl$_2$. The rational synthesis of this compound is described below.

^{1}H NMR (C_6D_6): δ = 1.03, 1.05 (2 s, 2 × 9H, CH$_2$C*Me*$_3$), 1.15 (s, 18H, cyclopentadienyl CCMe$_3$), 1.75, 1.80, 2.30, 2.39 (4 m, 4 × 2H, COD CH$_2$), 3.44 (m, 2H, COD CH *trans* to Cl), 3.62, 3.67, 3.80, 3.84, 4.11, 4.19 (6 m, 6 × 1H, cyclopentadienyl CH), 5.18, 5.21 (2 d, $^{2}J_{HH}$ = 13.6 Hz, 2 × 1H, C*H*^{A}H^{X}CMe$_3$), 4.41 (m, 2H, COD CH *cis* to Cl), 5.72, 5.73 (2 d, $^{2}J_{HH}$ = 13.6 Hz, 2 × 1H, CH^{A}*H*^{X}CMe$_3$). ^{13}C{^{1}H} NMR (C_6D_6): δ = 29.4 (m, 2 × COD CH$_2$), 29.5, 29.6 (2 × CH$_2$C*Me*$_3$), 30.01, 30.04 (2 × cyclopentadienyl C*C*Me$_3$), 31.6, 31.7 (2 × cyclopentadienyl CC*Me*$_3$), 31.9, 32.1 (2 × CH$_2$*C*Me$_3$), 32.7 (d, $^{2}J_{RhC}$ = 1.2 Hz, COD CH$_2$), 32.9 (br., COD CH$_2$), 64.2, 65.2, 65.4, 66.6, 68.1, 68.2 (6 × cyclopentadienyl CH), 69.1 (d, $^{1}J_{RhC}$ = 14.6 Hz, COD CH *trans* to Cl), 72.2, 72.3 (2 × *C*H$_2$CMe$_3$), 94.2 (d, $^{1}J_{RhC}$ = 7.7 Hz, COD CH *cis* to Cl), 98.9, 99.0 (2 d, $^{3}J_{RhC}$ = 1.3 Hz, cyclopentadienyl CN), 104.3, 104.5 (2 × cyclopentadienyl *C*CMe$_3$), 228.4 (d, $^{1}J_{RhC}$ = 47 Hz, carbene C). HRMS/ESI(+): *m*/*z* = 689.2984 [M−Cl]$^+$; 689.3004 calcd for [$C_{37}H_{58}FeN_2Rh$]$^+$.

Anal. Calcd for $C_{37}H_{58}ClFeN_2Rh$ (725.09): C, 61.29; H, 8.06; N, 3.86. Found: C, 61.07; H, 8.25; N, 3.60.

cis-[RhCl(A′-Np)(CO)$_2$]. A solution of *cis*-[RhCl(**A′-Np**)(COD)] (71.0 mg, 0.098 mmol) in C_6D_6 (2 mL) was stirred under an atmosphere of CO for 2 h. Completion of the reaction was confirmed by ^{1}H NMR spectroscopy. The solvent was stripped off *in vacuo*, affording the product as a yellow, air-sensitive solid in essentially quantitative yield. The crude product contained small amounts of unidentified Rh species and trace amounts of residual solvent, which could not be removed. All attempts to obtain the compound in crystalline form and analytical purity failed.

^{1}H NMR (C_6D_6): δ = 0.96, 0.99 (2 s, 2 × 9H, CH$_2$C*Me*$_3$), 1.00 (s, 18H, cyclopentadienyl CCMe$_3$), 3.64 (d, $^{2}J_{HH}$ = 14.5 Hz, 1H, C^{A}*H*^{A}H^{X}CMe$_3$), 3.74 (d, $^{2}J_{HH}$ = 14.1 Hz, 1H, C^{B}*H*^{A}H^{X}CMe$_3$), 3.80 (m, 2H, CH), 3.81, 3.85, 3.97, 4.14 (4 m, 4 × 1H, CH), 5.91 (d, $^{2}J_{HH}$ = 14.1 Hz, 1H, C^{B}H^{A}*H*^{X}CMe$_3$), 6.03 (d, $^{2}J_{HH}$ = 14.5 Hz, 1H, C^{A}H^{A}*H*^{X}CMe$_3$). ^{13}C{^{1}H} NMR (C_6D_6): δ = 29.1, 29.3 (2 × CH$_2$C*Me*$_3$), 30.0, 30.1 (2 × cyclopentadienyl C*C*Me$_3$), 31.62, 31.64 (2 × cyclopentadienyl CC*Me*$_3$), 32.7, 32.8 (2 × CH$_2$*C*Me$_3$), 64.3, 64.8, 65.7, 65.8, 68.3, 68.9 (6 × CH), 73.1, 73.5 (2 × *C*H$_2$CMe$_3$), 98.3 (d, $^{3}J_{RhC}$ = 1.4 Hz, cyclopentadienyl CN), 98.9 (d, $^{3}J_{RhC}$ = 1.5 Hz, cyclopentadienyl CN), 104.4, 105.2 (2 × cyclopentadienyl *C*CMe$_3$), 185.2 (d, $^{1}J_{RhC}$ = 76 Hz, CO), 187.7 (d, $^{1}J_{RhC}$ = 55 Hz, CO), 215.5 (d, $^{1}J_{RhC}$ = 41 Hz, carbene C). IR (CH_2Cl_2): ν_{CO} = 2076, 1998.

Carbonylation of A′-Np. A solution of **A′-Np** (125 mg, 0.26 mmol) in C_6D_6 (1.0 mL) was prepared in a silylated Schlenk flask. The solution was degassed by three freeze−pump−thaw cycles. At the end of the last cycle, CO was introduced into the flask and the solution stirred under a slight flow of CO for 1.5 h. Completion of the reaction was confirmed by ^{1}H NMR spectroscopy, which indicated the formation of (**A′-Np**)$_2$CO as a mixture of isomers, contaminated with a small amount of hydrolysis products.

^{1}H NMR (C_6D_6): δ = 0.85−1.42 (numerous s, CMe$_3$), 2.30−4.61 (numerous overlapping m, CH$_2$ and CH), 4.91−5.32 (several overlapping d, $^3J_{HH}$ ≈ 13.8 Hz, CH$_2$). An unambiguous assignment of resonances was not possible due to overlapping resonances and an only approximately known ratio of isomers, together with the presence of a small amount of hydrolysis product. See the Supporting Information (Figure S42) for the complete ^{1}H NMR spectrum. A small amount of crystals was obtained from a hexane solution of this mixture of isomers after several weeks. One of them turned out to be suitable for a single-crystal XRD study, which revealed that it contained the two enantiomers (R_pR_p-**A′-Np**)═C(O$^-$)(R_pR_p-**A′-Np**$^+$) and (S_pS_p-**A′-Np**)═C(O$^-$)(S_pS_p-**A′-Np**$^+$) as a racemic compound. The other crystals were subjected to NMR spectroscopic analysis.

^{1}H NMR (C_6D_6): δ = 0.93, 0.99, 1.03, 1.06, 1.14, 1.15, 1.20, 1.22, 1.28, 1.31, 1.32, 1.33, 1.34, 1.42, 1.43, 1.45, (16 s, 16 × 9H, CMe$_3$), 3.05, 3.06, 3.14, 3.17, 3.27, 3.31, 3.35, 3.41 (8 d, $^2J_{HH}$ = 13.8 Hz, 8 × 1H, $C\mathit{H}^{A}H^{X}CMe_3$), 3.48−3.56 (m, 4H, $CH^{A}\mathit{H}^{X}CMe_3$), 3.57, 3.62 (2 m, 2 × 1H, CH), 3.79 (m, 2H, CH), 3.86 (m, 1H, CH), 3.88 (m, 4H, CH), 3.92, 3.93, 3.96, 3.99, 4.03, 4.06 (6 m, 6 × 1H, CH), 4.08 (br. s, 1H, CH), 4.32, 4.36, 4.37, 4.40 (4 m, 4 × 1H, CH), 4.44−4.47 (m, 2H, CH), 4.51 (br. s, 1H, CH), 4.54 (m, 1H, CH), 5.09, 5.13, 5.28, 5.38 (4 d, $^2J_{HH}$ = 13.8 Hz, 4 × 1H, $C\mathit{H}^{A}H^{X}CMe_3$). ^{13}C{^{1}H} NMR ($C_6D_6$): δ = 27.8, 29.4, 29.6, 30.1, 30.2, 30.3, 31.3, 31.4, 31.6, 31.8, 32.2, 32.3, 32.6, 57.4, 58.3, 59.3, 59.6 (br.), 61.1 (br.), 62.9 (br.), 64.9, 65.0 (br.), 65.3 (br.), 65.5 (br.), 65.8, 66.0, 66.5 (br.), 66.8, 67.6, 67.9, 68.5 (br.), 68.8, 69.1, 69.4, 69.6, 70.2, 70.3, 70.6, 71.1, 71.2, 72.2, 93.8, 95.0, 96.3 (br.), 96.6 (br.), 97.8 (br.), 100.9 (br.), 101.2 (br.), 104.0 (br.), 105.1 (br.), 105.7, 107.0 (br.), 136.6 (br.), 148.0 (br.), 177.6 (br.). Because of the complexity of the spectrum and the presence of numerous broad signals, an assignment was not possible. HRMS/ESI(+): m/z = 985.6014 [M + H]$^+$; 985.6048 calcd for [$C_{59}H_{93}Fe_2N_4O$]$^+$.

A′-NpH−CHCl$_2$. Dichloromethane (50 μL, 0.78 mmol) was added to a solution of **A′-Np** (57 mg, 0.12 mmol) in C_6D_6 (0.6 mL). The reaction was complete within <10 min, according to ^{1}H NMR spectroscopic analysis. Volatile components were subsequently removed *in vacuo* and the product crystallized from a minimal amount of acetonitrile, affording yellow crystals. The crystal used for a single-crystal XRD study was taken from this batch. Yield: 32 mg (47%).

^{1}H NMR (CDCl$_3$): δ = 0.94, 0.97 (2 s, 2 × 9H, CH$_2$C*Me*$_3$), 1.14, 1.16 (2 s, 2 × 9H, cyclopentadienyl CCMe$_3$), 2.74 (d, $^2J_{HH}$ = 13.5 Hz, 1H, $C^{A}\mathit{H}^{A}H^{X}CMe_3$), 2.77 (d, $^2J_{HH}$ = 14.0 Hz, 1H, $C^{B}\mathit{H}^{A}H^{X}CMe_3$), 2.91 (d, $^2J_{HH}$ = 13.5 Hz, 1H, $C^{A}H^{A}\mathit{H}^{X}CMe_3$), 3.01 (d, $^2J_{HH}$ = 14.0 Hz, 1H, $C^{B}H^{A}\mathit{H}^{X}CMe_3$), 3.10, 3.13, 3.79, 3.95 (4 m, 4 × 1H, CH), 4.08−4.09 (m, 2H, CH), 4.81 (d, $^2J_{HH}$ = 9.5 Hz, 1H, N$_2$CH), 6.09 (d, $^2J_{HH}$ = 9.5 Hz, 1H, Cl$_2$CH). ^{13}C{^{1}H} NMR (CDCl$_3$): δ = 28.7, 29.1 (2 × CH$_2$C*Me*$_3$), 30.0, 30.1 (2 × cyclopentadienyl CCMe$_3$), 31.7, 32.0 (2 × cyclopentadienyl CC*Me*$_3$), 35.1, 35.2 (2 × CH$_2$CMe$_3$), 59.3, 60.1 (2 × CH$_2$), 62.6, 66.3, 66.9, 67.2, 68.0, 68.3 (6 × CH), 75.2 (Cl$_2$CH), 97.0 (cyclopentadienyl CN), 97.96, 98.01 (cyclopentadienyl CN and cyclopentadienyl CCMe$_3$), 102.5 (cyclopentadienyl CCMe$_3$), 103.0 (N$_2$CH). HRMS/ESI(+): m/z = 562.2545 [M]$^+$; 562.2544 calcd for [$C_{30}H_{48}Cl_2FeN_2$]$^+$.

Anal. Calcd for $C_{30}H_{48}Cl_2FeN_2$ (563.48): C, 58.56; H, 7.15; N, 6.21. Found: C, 58.91; H, 7.17; N, 6.26.

A-NpH−CHCl$_2$. Dichloromethane (0.5 mL, 7.8 mmol) was added to a solution of **A-Np** (106 mg, 0.29 mmol) in diethyl ether (3.0 mL). The reaction was complete within <10 min, according to ^{1}H NMR spectroscopic analysis. Volatile components were subsequently removed *in vacuo* and the product crystallized from ethanol. The crystal used for a single-crystal XRD study was taken from this batch. Yield: 81 mg (62%).

^{1}H NMR (CDCl$_3$): δ = 0.96 (s, 18H, CMe$_3$), 2.83, 2.98 (2 d, $^2J_{HH}$ = 14.0 Hz, 2 × 2H, $C\mathit{H}^{A}\mathit{H}^{B}Me_3$), 3.28, 3.91, 4.11, 4.24 (4 m, 4 × 2 H, CH), 4.87 (d, $^3J_{HH}$ = 9.6 Hz, 1H, N$_2$CH), 6.16 (d, $^3J_{HH}$ = 9.6 Hz, 1H, Cl$_2$CH). ^{13}C{^{1}H} NMR (CDCl$_3$): δ = 28.9 (C*Me*$_3$), 35.3 (CMe$_3$), 62.3 64.8 (2 × CH), 68.0 (CH$_2$), 68.9, 70.2 (2 × CH), 75.1 (Cl$_2$CH), 99.0 (cyclopentadienyl CN), 103.0 (N$_2$CH) ppm. HRMS/ESI(+): m/z = 450.1286 [M]$^+$; 450.1292 calcd for [$C_{22}H_{32}Cl_2FeN_2$]$^+$.

Anal. Calcd for $C_{22}H_{32}Cl_2FeN_2$ (451.26): C, 58.56; H, 7.15; N, 6.21. Found: C, 58.91; H, 7.17; N, 6.26.

A-Np(H$_2$O). Water (10 μL, 0.56 mmol) was added to a stirred solution of **A-Np** (54 mg, 0.15 mmol) in THF (3.0 mL), whereupon the yellow solution immediately turned orange. After 2 h, volatile components were removed *in vacuo*, leaving the product as an orange solid. Yield: 57 mg (100%). HRMS/ESI(+): m/z = 384.1869 [M]$^+$; 384.1864 calcd for [$C_{21}H_{32}FeN_2O$]$^+$.

Anal. Calcd for $C_{21}H_{32}N_2FeO$ (384.34): C, 65.63; H, 8.39; N, 7.29. Found: C, 65.79; H, 8.76; N, 7.22.

According to NMR spectroscopic analysis, the product consists of the *E* and *Z* isomer of [Fe{η^5-C$_5$H$_4$[NNp(CHO)]}{η^5-C$_5$H$_4$(NHNp)}], which are present in a solvent-dependent equilibrium, as is typically observed for tertiary formamides due to the partial double bond character of the amide C(O)−N bond.[45,46]

NMR data for the major isomer:

^{1}H NMR (C_6D_6): δ = 0.86 (s, 18H, CH$_2$C*Me*$_3$), 2.09 (t, $^3J_{HH}$ = 6.9 Hz, 1H, NH), 2.52 (d, $^3J_{HH}$ = 6.9 Hz, 2H, NHC*H*$_2$CMe$_3$), 3.52 (s, 2H, N(CHO)C*H*$_2$CMe$_3$), 3.58, 3.71, 3.83, 3.95 (4 m, 4 × 2H, cyclopentadienyl CH), 9.24 (s, 1H, CHO). ^{13}C{^{1}H} NMR (C_6D_6): δ = 27.7, 28.6 (2 × CH$_2$C*Me*$_3$), 31.6, 33.8 (2 × CH$_2$CMe$_3$), 56.3, 56.6, 59.2, 63.5, 64.4, 65.4 (2 × CH$_2$, 4 × cyclopentadienyl CH), 101.3, 113.5 (2 × cyclopentadienyl CN), 164.6 (CHO).

^{1}H NMR (CD$_2$Cl$_2$): δ = 0.77, 0.94 (2 s, 2 × 9H, CH$_2$C*Me*$_3$), 2.40 (t, $^3J_{HH}$ = 6.7 Hz, 1H, NH), 2.65 (d, $^3J_{HH}$ = 6.7 Hz, 2H, NHC*H*$_2$CMe$_3$), 3.37 (s, 2H, N(CHO)C*H*$_2$CMe$_3$), 3.82, 3.87, 4.07, 4.21 (4 m, 4 × 2H, cyclopentadienyl CH), 9.09 (s, 1H, CHO). ^{13}C{^{1}H} NMR (CD$_2$Cl$_2$): δ = 27.7, 28.4 (2 × CH$_2$C*Me*$_3$), 31.6, 33.8 (2 × CH$_2$CMe$_3$), 56.4, 56.5, 59.5, 63.8, 64.6, 65.7 (2 × CH$_2$, 4 × cyclopentadienyl CH), 101.1, 113.4 (2 × cyclopentadienyl CN), 165.0 (CHO).

^{1}H NMR (THF-*d*$_8$): δ = 0.76, 0.93 (2 s, 2 × 9H, CH$_2$C*Me*$_3$), 2.67 (d, $^3J_{HH}$ = 6.7 Hz, 2H, NHC*H*$_2$CMe$_3$), 3.37 (br.s, 1H, NH), 3.38 (s, 2H, N(CHO)C*H*$_2$CMe$_3$), 3.79 (m, 4H cyclopentadienyl CH), 4.02, 4.22 (2 m, 2 × 2H, cyclopentadienyl CH), 9.06 (s, 1H, CHO). ^{13}C{^{1}H} NMR (THF-*d*$_8$): δ = 27.9, 28.8 (2 × CH$_2$C*Me*$_3$), 32.3, 34.2 (2 × CH$_2$CMe$_3$), 56.3, 56.5, 59.7, 63.8, 64.4, 65.7 (2 × CH$_2$, 4 × cyclopentadienyl CH), 101.9, 115.1 (2 × cyclopentadienyl CN), 164.7 (CHO).

NMR data for the minor isomer:

^{1}H NMR (C_6D_6): δ = 0.57, 1.10 (2 s, 2 × 9H, CH$_2$C*Me*$_3$), 2.81 (s, 2H, N(CHO)C*H*$_2$CMe$_3$), 2.82 (d, $^3J_{HH}$ = 6.7 Hz, 2H, NHC*H*$_2$CMe$_3$), 3.72 (t, $^3J_{HH}$ = 6.7 Hz, 1H, NH), 3.90 (m, 4H, cyclopentadienyl CH), 3.97, 4.49 (2 m, 2 × 2H, cyclopentadienyl CH), 7.99 (s, 1H, CHO). ^{13}C{^{1}H} NMR (C_6D_6): δ = 27.8, 28.2 (2 × CH$_2$C*Me*$_3$), 31.7, 33.2 (2 × CH$_2$CMe$_3$), 58.3, 59.5, 60.3, 62.8, 63.9, 64.5 (2 × CH$_2$, 4 × cyclopentadienyl CH), 98.8, 113.8 (2 × cyclopentadienyl CN), 162.3 (CHO).

^{1}H NMR (CD$_2$Cl$_2$): δ = 0.81, 0.97 (2 s, 2 × 9H, CH$_2$C*Me*$_3$), 2.66 (d, $^3J_{HH}$ = 6.9 Hz, 2H, NHC*H*$_2$CMe$_3$), 3.05 (t, $^3J_{HH}$ = 6.9 Hz, 1H, NH), 3.32 (s, 2H, N(CHO)C*H*$_2$CMe$_3$), 3.74, 3.82, 4.00, 4.47 (4 m, 4 × 2H, cyclopentadienyl CH), 8.19 (s, 1H, CHO). ^{13}C{^{1}H} NMR (CD$_2$Cl$_2$): δ = 27.9, 28.0 (2 × CH$_2$C*Me*$_3$), 31.6, 33.6 (2 × CH$_2$CMe$_3$), 57.6, 59.5, 60.8, 62.9, 64.0, 64.5 (2 × CH$_2$, 4 × cyclopentadienyl CH), 98.6, 113.2 (2 × cyclopentadienyl CN), 162.8 (CHO).

^{1}H NMR (THF-*d*$_8$): δ = 0.80, 0.97 (2 s, 2 × 9H, CH$_2$C*Me*$_3$), 2.68 (d, $^3J_{HH}$ = 6.7 Hz, 2H, NHC*H*$_2$CMe$_3$), 3.52 (t, $^3J_{HH}$ = 6.7 Hz, 1H, NH), 3.41 (s, 2H, N(CHO)C*H*$_2$CMe$_3$), 3.69, 3.73, 3.94, 4.49 (4 m, 4 × 2H, cyclopentadienyl CH), 8.19 (s, 1H, CHO). ^{13}C{^{1}H} NMR (THF-*d*$_8$): δ = 28.1, 28.2 (2 × CH$_2$C*Me*$_3$), 32.1, 34.0 (2 × CH$_2$CMe$_3$), 57.9, 59.8, 60.5, 63.1, 64.0, 64.6 (2 × CH$_2$, 4 × cyclopentadienyl CH), 99.4, 114.3 (2 × cyclopentadienyl CN), 163.1 (CHO).

X-ray Crystallography. For each data collection a single crystal was mounted on a glass fiber and all geometric and intensity data were taken from this sample. Data collection using Mo Kα radiation (λ = 0.71073 Å) was made with a Stoe IPDS2 diffractometer equipped with a two-circle goniometer and an area detector. The datasets were corrected for absorption, Lorentz, and polarization effects. The structures were solved by direct methods (SIR 2008)[50] and refined using alternating cycles of least-squares refinements against F^2 (SHELXL2014/7).[51] H atoms were included in the models in calculated positions with the 1.2-fold isotropic displacement parameter of their bonding partner. For compound [**A′-NpH**]$\mathrm{BF_4}$, a non-resolvable solvent molecule has been removed using the SQUEEZE routine from PLATON.[52] Experimental details for each diffraction experiment are given in Table S1 in the Supporting Information. Data for all compounds have been deposited with the Cambridge Crystallographic Database (see deposition numbers listed in Table S1 in the Supporting Information).

■ ASSOCIATED CONTENT

Ⓢ Supporting Information

Crystallographic data (including CIF files) for compounds **3**, **4**, **5**, [**A′-NpH**]$\mathrm{BF_4}$, the racemic compound ($R_\mathrm{p}R_\mathrm{p}$-**10**)═C(O$^-$)($R_\mathrm{p}R_\mathrm{p}$-**10**$^+$)/($S_\mathrm{p}S_\mathrm{p}$-**10**)═C(O$^-$)($S_\mathrm{p}S_\mathrm{p}$-**10**$^+$), **A′-NpH**−$\mathrm{CHCl_2}$, **A-NpH**−$\mathrm{CH_2CN}$, **A-NpH**−$\mathrm{CHCl_2}$, and **10**. Molecular structure diagrams of **A-NpH**−$\mathrm{CH_2CN}$, **A-NpH**−$\mathrm{CHCl_2}$, and **10**. Cyclic voltammograms of **1**, **8**, **9**, [**A′-NpH**]$\mathrm{BF_4}$, and the hydrolysis products of **A-Np**; square wave voltammogram of **9**. EPR spectrum of the hydrolysis products of **A-Np**. Plots of NMR spectra for *tert*-butylcyclopentadiene and all new compounds. Computational details for **A-Np** (singlet, triplet) and **A′-Np** (singlet, triplet) including Cartesian coordinates and total energies. The Supporting Information is available free of charge on the ACS Publications website at DOI: 10.1021/acs.inorgchem.5b01064.

■ AUTHOR INFORMATION

Corresponding Author

*E-mail: siemeling@uni-kassel.de.

Notes

The authors declare no competing financial interest.

■ ACKNOWLEDGMENTS

The authors are grateful to Umicore AG&Co. KG (Hanau, Germany) for a generous gift of precious metal compounds, to Dr. Christian Färber, Dr. Pavel Turek, and Michél Liebscher for preliminary synthetic investigations, and to Dr. Daniel Weismann for his assistance in the electrochemical study. The authors thank one of the referees for helpful comments.

■ DEDICATION

Dedicated to Prof. Manfred Scheer on the occasion of his 60th birthday.

■ REFERENCES

(1) For recent reviews, see: (a) *N-Heterocyclic Carbenes−Effective Tools for Organometallic Synthesis*; Nolan, S. P., Ed.; Wiley−VCH: Weinheim, Germany, 2014. (b) Hopkinson, M. N.; Richter, C.; Schedler, M.; Glorius, F. *Nature* **2014**, *510*, 485−496.

(2) For a recent review, see: Li, J.; Shen, W.-X.; Li, X.-R. *Curr. Org. Chem.* **2012**, *16*, 2879−2891.

(3) For selected recent examples, see: (a) Yang, L.; Zhang, X.; Mao, P.; Xiao, Y.; Bian, H.; Yuan, J.; Mai, W.; Qu, L. *RSC Adv.* **2015**, *5*, 25723−25729. (b) Phillips, N.; Dodson, T.; Tirfoin, R.; Bates, J. I.; Aldridge, S. *Chem.—Eur. J.* **2014**, *20*, 16721−16731. (c) Phillips, N.; Tirfoin, R.; Aldridge, S. *Dalton Trans.* **2014**, *43*, 15279−15282. (d) Phillips, N.; Treasure, L.; Rees, N. H.; Tirfoin, R.; McGrady, J. E.; Aldridge, S. *Eur. J. Inorg. Chem.* **2014**, 4877−4885. (e) Collins, L. R.; Rookes, T. M.; Mahon, M. F.; Riddlestone, I. M.; Whittlesey, M. K. *Organometallics* **2014**, *33*, 5882−5887. (f) Yang, B.-M.; Xiang, K.; Tu, Y.-Q.; Zhang, S.-H.; Yang, D.-T.; Wang, S.-H.; Zhang, F.-M. *Chem. Commun.* **2014**, *50*, 7163−7165. (g) Poulten, R. C.; López, I.; Llobet, A.; Mahon, M.-F.; Whittlesey, M. K. *Inorg. Chem.* **2014**, *53*, 7160−7169. (h) Blase, V.; Flores-Figueroa, A.; Schulte to Brinke, C.; Hahn, F. E. *Organometallics* **2014**, *33*, 4471−4478. (i) Dunsford, J. J.; Cavell, K. J. *Organometallics* **2014**, *33*, 2903−2905. (j) Mozorov, O. S.; Lunchev, A. V.; Bush, A. A.; Tukov, A. A.; Asachenko, A. F.; Khrustalev, V. N.; Zalesskiy, S. S.; Ananikov, V. P.; Nechaev, M. S. *Chem.—Eur. J.* **2014**, *20*, 6162−6170. (k) Phillips, N.; Tirfoin, R.; Aldridge, S. *Chem.—Eur. J.* **2014**, *20*, 3825−3830. (l) Huang, L.; Cao, Y.; Zhao, M.; Tang, Z.; Sun, Z. *Org. Biomol. Chem.* **2014**, *12*, 6554−6556. (m) Dunsford, J. J.; Cade, I. A.; Fillman, K. L.; Neidig, M. L.; Ingleson, M. J. *Organometallics* **2014**, *33*, 370−377.

(4) For reviews, see: (a) Vignolle, J.; Cattoën, X.; Bourissou, D. *Chem. Rev.* **2009**, *109*, 3333−3384. (b) Alder, R. W.; Blake, M. E.; Chaker, L.; Harvey, J. N.; Paolini, F.; Schütz, J. *Angew. Chem., Int. Ed.* **2004**, *43*, 5896−5911.

(5) Frey, N.; Haddow, M. F.; Harvey, J. N.; McMullin, C. L.; Orpen, A. G. *Dalton Trans.* **2009**, 8183−8196.

(6) (a) Nelson, D. J.; Nolan, S. P. *Chem. Soc. Rev.* **2013**, *42*, 6723−6753. (b) Dröge, T.; Glorius, F. *Angew. Chem., Int. Ed.* **2010**, *49*, 6940−6952.

(7) For a review, see: Siemeling, U. *Eur. J. Inorg. Chem.* **2012**, 3523−3536.

(8) (a) Rittinghaus, S.; Färber, C.; Bruhn, C.; Siemeling, U. *Dalton Trans.* **2014**, *43*, 3508−3520. (b) Siemeling, U.; Färber, C.; Leibold, M.; Bruhn, C.; Mücke, P.; Winter, R. F.; Sarkar, B.; von Hopffgarten, M.; Frenking, G. *Eur. J. Inorg. Chem.* **2009**, 4607−4612. (c) Siemeling, U.; Färber, C.; Bruhn, C. *Chem. Commun.* **2009**, 98−100.

(9) (a) Varnado, C. D.; Rosen, E. L., Jr.; Collins, M. S.; Lynch, V. M.; Bielawski, C. W. *Dalton Trans.* **2013**, *42*, 13251−13264. (b) Khramov, D. M.; Rosen, E. L.; Lynch, V. M.; Bielawski, C. W. *Angew. Chem., Int. Ed.* **2008**, *47*, 2267−2270.

(10) (a) Siemeling, U. *Aust. J. Chem.* **2011**, *64*, 1109−1112. (b) Goedecke, C.; Leibold, M.; Siemeling, U.; Frenking, G. *J. Am. Chem. Soc.* **2011**, *133*, 3557−3569. (c) Siemeling, U.; Färber, C.; Bruhn, C.; Leibold, M.; Selent, D.; Baumann, W.; von Hopffgarten, M.; Goedecke, C.; Frenking, G. *Chem. Sci.* **2010**, *1*, 697−704.

(11) Martin, D.; Moore, C. E.; Rheingold, A. L.; Bertrand, G. *Angew. Chem., Int. Ed.* **2013**, *52*, 7014−7017.

(12) Rosen, E. L.; Varnado, C. D., Jr; Tennyson, A. G.; Khramov, D. M.; Kamplain, J. W.; Sung, D. H.; Cresswell, P. T.; Lynch, V. M.; Bielawski, C. W. *Organometallics* **2009**, *28*, 6695−6706.

(13) Ramnial, T.; McKenzie, I.; Gorodetzki, B.; Tsang, E. M. W.; Clyburne, J. A. C. *Chem. Commun.* **2004**, 1054−1055.

(14) Masson, G.; Beyer, P.; Cyr, P. W.; Lough, A. J.; Manners, I. *Macromolecules* **2006**, *39*, 3720−3730.

(15) Seminal papers: (a) Schlögl, K.; Fried, M. *Monatsh. Chem.* **1964**, *95*, 558−575. (b) Falk, H.; Schlögl, K. *Monatsh. Chem.* **1965**, *96*, 266−275. (c) For reviews, see: Wagner, G.; Herrmann, R. In *Ferrocenes: Homogeneous Catalysis, Organic Synthesis, Materials Science*; Togni, A., Hayashi, T., Eds.; VCH: Weinheim, Germany, 1995; pp 173−218. (d) Schlögl, K. *Top. Stereochem.* **1967**, *1*, 39−92.

(16) (a) Morrison, C. A.; Bone, S. F.; Rankin, D. W. H.; Robertson, H. E.; Parsons, S.; Coxall, R. A.; Fraser, S.; Howell, J. A. S.; Yates, P. C.; Fey, N. *Organometallics* **2001**, *20*, 2309−2320. (b) Herberhold, M.; Cheng, Y.-X.; Jin, G.-X.; Milius, W. *Z. Naturforsch. B: Chem. Sci.* **2000**, *55*, 814−820. (c) Compton, D. L.; Rauchfuss, T. B. *Organometallics* **1994**, *13*, 4367−4376. (d) Köhler, F. H.; Geike, W. A.; Hertkorn, N. *J. Organomet. Chem.* **1987**, *334*, 359−367.

(17) For a closely related case, see: Petrov, A. R.; Jess, K.; Freytag, M.; Jones, P. G.; Tamm, M. *Organometallics* **2013**, *32*, 5946−5954.

(18) Roemer, M.; Heinrich, D.; Kang, Y. K.; Chung, Y. K.; Lentz, D. *Organometallics* **2012**, *31*, 1500−1510.

(19) (a) Sänger, I.; Heilmann, J. B.; Bolte, M.; Lerner, H.-W.; Wagner, M. *Chem. Commun.* **2006**, 2027−2029. (b) Butler, I. R.; Cullen, W. R.; Rettig, J.; Ni, S. R. *Organometallics* **1985**, *4*, 2196−2201.

(20) Shafir, A.; Power, M. P.; Whitener, G. D.; Arnold, J. *Organometallics* **2000**, *19*, 3978−3982.

(21) Otón, F.; Espinosa, A.; Tárraga, A.; Ramírez de Aranello, C.; Molina, P. *Chem.—Eur. J.* **2007**, *13*, 5742−5752.

(22) Nudelman, A.; Bechor, Y.; Falb, E.; Fischer, B.; Wexler, B. A.; Nudelman, A. *Synth. Commun.* **1998**, *28*, 471−474.

(23) Boese, R.; Bläser, D.; Kuhn, N.; Stubenrauch, S. *Z. Kristallogr.* **1993**, *205*, 282−284.

(24) Okuda, J.; Herdtweck, E. *J. Organomet. Chem.* **1989**, *373*, 99−105.

(25) Hoffman, R. V. *Organic Chemistry*; 2nd Edition; Wiley: Hoboken, NJ, 2004; p 167.

(26) Martin, D.; Soleilhavoup, M.; Bertrand, G. *Chem. Sci.* **2011**, *2*, 389−399.

(27) Moss, R. A.; Krogh-Jespersen, K. *Tetrahedron Lett.* **2013**, *54*, 4303−4305 and references cited therein..

(28) Mendez, F.; Garcia-Garibay, M. A. *J. Org. Chem.* **1999**, *64*, 7061−7066.

(29) Bach, R. D.; Su, M.-D.; Aldabbagh, E.; Andrés, J. L.; Schlegel, H. B. *J. Am. Chem. Soc.* **1993**, *115*, 10237−10246.

(30) (a) Moerdyk, J. P.; Bielawski, C. W. In *Contemporary Carbene Chemistry*; Moss, R. A., Doyle, M. P., Eds.; Wiley: Hoboken, NJ, 2014; pp 40−74. (b) Moerdyk, J. P.; Bielawski, C. W. *Nat. Chem.* **2012**, *4*, 275−280. (c) Hudnall, T. W.; Moorhead, E. J.; Gusev, D. G.; Bielawski, C. W. *J. Org. Chem.* **2010**, *75*, 2763−2766. (d) Kassaee, M. Z.; Ghambarian, M.; Shakib, F. A.; Momeni, M. R. *J. Phys. Org. Chem.* **2010**, *24*, 351−359.

(31) Anslyn, E. V.; Dougherty, D. A. *Modern Physical Organic Chemistry*; University Science Books: Sausalito, CA, 2006; p 22.

(32) (a) Mormul, J.; Steimann, M.; Maichle-Mössmer, C.; Nagel, U. *Eur. J. Inorg. Chem.* **2013**, 3421−3428. (b) Korotkikh, N. I.; Raenko, G. F.; Pekhtereva, T. M.; Shvaika, O. P.; Cowley, A. H.; Jones, J. N. *Russ. J. Org. Chem.* **2006**, *42*, 1822−1833. (c) Arduengo, A. J., III; Calabrese, J. C.; Davidson, F.; Dias, H. V. R.; Goerlich, J. R.; Krafczyk, R.; Marshall, W. J.; Tamm, M.; Schmutzler, R. *Helv. Chim. Acta* **1999**, *82*, 2348−2364.

(33) (a) Born, M.; Ingemann, S.; Nibbering, N. M. M. *Int. J. Mass Spectrom.* **2000**, *194*, 103−113. (b) Bohme, D. K.; Lee-Ruff, E.; Young, L. B. *J. Am. Chem. Soc.* **1972**, *94*, 5153−5159.

(34) Zhong, Z.-H.; Matsumura-Inoue, T.; Ichimura, A. *Anal. Sci.* **1992**, *8*, 877−879.

(35) Okuda, J.; Albach, R. W.; Herdtweck, E.; Wagner, F. E. *Polyhedron* **1991**, *10*, 1741−1748.

(36) Maekawa, M.; Daniliuc, C. G.; Freytag, M.; Jones, P. G.; Walter, M. D. *Dalton Trans.* **2012**, *41*, 10317−10327.

(37) Slocum, D. W.; Ernst, C. R. Electronic Effects in Metallocenes and Certain Related Systems. In *Advances in Organometallic Chemistry*; Stone, F. G. A., Robert, W., Eds.; Academic Press: New York, 1972; Vol. *10*, pp 79−114.

(38) Gassman, P. G.; Macomber, D. W.; Hershberger, J. W. *Organometallics* **1983**, *2*, 1470−1472.

(39) Lu, S.; Strelets, V. V.; Ryan, M. F.; Pietro, W. J.; Lever, A. B. P. *Inorg. Chem.* **1996**, *35*, 1013−1023.

(40) Prins, R.; Korswagen, A. R. *J. Organomet. Chem.* **1970**, *25*, C74−C76.

(41) Neidlinger, A.; Ksenofontov, V.; Heinze, K. *Organometallics* **2013**, *32*, 5955−5965.

(42) Kowalski, K.; Linseis, M.; Winter, R. F.; Zabel, M.; Záliš, S.; Kelm, H.; Krüger, H.-J.; Sarkar, B.; Kaim, W. *Organometallics* **2009**, *28*, 4196−4209.

(43) Kramer, J. A.; Hendrickson, D. N. *Inorg. Chem.* **1980**, *19*, 3330−3337.

(44) For a study addressing the hydrolysis of NHCs in detail, see: Hollóczki, O.; Terleczky, P.; Szieberth, D.; Mourgas, G.; Gudat, D.; Nyulászi, L. *J. Am. Chem. Soc.* **2011**, *133*, 780−789.

(45) For a review, see: Steward, W. E.; Siddal, T. H., III. *Chem. Rev.* **1970**, *70*, 517−551.

(46) For an NMR study addressing the *E*/*Z* conformational equilibrium of tertiary aryl formamides, see: Leis, J.; Klika, K. D.; Karelson, M. *Tetrahedron* **1998**, *54*, 7497−7504.

(47) See, for example: Lacour, J.; Hebbe-Viton, V. *Chem. Soc. Rev.* **2003**, *32*, 373−382.

(48) (a) Paradies, J.; Kehr, G.; Fröhlich, R.; Erker, G. *Proc. Natl. Acad. Sci. U.S.A.* **2006**, *103*, 15333−15337. (b) Riemschneider, R.; Reisch, A.; Horak, H. *Monatsh. Chem.* **1960**, *91*, 805−811.

(49) Nichols, M. A.; Williard, P. G. *J. Am. Chem. Soc.* **1993**, *115*, 1568−1572.

(50) Burla, M. C.; Caliandro, R.; Camalli, M.; Carrozzini, B.; Cascarano, G. L.; De Caro, L.; Giacovazzo, C.; Polidori, G.; Spagna, R. *J. Appl. Crystallogr.* **2007**, *40*, 609−613.

(51) Sheldrick, G. M. *Acta Crystallogr., Sect. A: Found. Crystallogr.* **2008**, *64*, 112−122.

(52) Spek, A. L. *Acta Crystallogr., Sect. D: Biol. Crystallogr.* **2009**, *65*, 148−155.